Environment International 144 (2020) 105990

Contents lists available at ScienceDirect

Environment International

journal homepage: www.elsevier.com/locate/envint

Odour impact assessment by considering short-term ambient concentrations: A multi-model and two-site comparison

Marzio Invernizzi[a,*], Marlon Brancher[b], Selena Sironi[a], Laura Capelli[a], Martin Piringer[c], Günther Schauberger[b]

[a] Politecnico di Milano, Department of Chemistry, Materials and Chemical Engineering "Giulio Natta", Piazza Leonardo da Vinci 32, 20133 Milan, Italy
[b] WG Environmental Health, Unit for Physiology and Biophysics, University of Veterinary Medicine, Veterinärplatz 1, A-1210 Vienna, Austria
[c] Department of Environmental Meteorology, Central Institute of Meteorology and Geodynamics, Hohe Warte 38, A-1190 Vienna, Austria

ARTICLE INFO

Handling Editor: Xavier Querol

Keywords:
Peak-to-mean
Lagrangian model
Separation distance
Dispersion modelling
Concentration fluctuation
Odour

ABSTRACT

Short-term events are one of the specific aspects that differentiate odour nuisance problems from conventional air quality pollutants. Atmospheric dispersion modelling has been considered the gold standard to realise odour impact assessments and to calculate separation distances. Most of these models provide predictions of concentrations of a pollutant in ambient air on an hourly basis. Even when the hourly mean odour concentration is lower than the perception threshold, concentration peaks above the threshold may occur during this period. The constant peak-to-mean factor is nowadays the most widespread method for evaluating short-term concentrations from the long-term ones. Different approaches have been proposed in the scientific literature to consider non-constant peak-to-mean factors. Two prominent approaches to do so are the i) variable peak-to-mean factor which considers the distance from the source and atmospheric stability and the ii) concentration-variance transport. In this sense, the aim of this work is to compare the results of three different freely available dispersion models (namely, CALPUFF, LAPMOD and GRAL), which implement three distinct ways to evaluate the short-term concentration values. Two sites, one in Austria and the other in Italy, were selected for the investigation.

Dispersion model results were compared and discussed both in terms of long-term (hourly) concentrations and short-term. An important outcome of this work is that the dispersion models provided more equivalent results for hourly mean concentrations, in particular in the far-field. On the contrary, the method to evaluate short-term concentrations can deliver disparate results, thereby revealing a potential risk of poor assessment conclusions.

The utilistion of a multiangle methodological approach (dispersion models, study site locations, algorithms to incorporate short-term concentrations) allowed providing useful information for future studies and policy-making in this field. Accordingly, our findings call for awareness on how the use of a particular dispersion model and its sub-hourly peak calculation method can affect odour impact assessment conclusions and compliance demonstrations.

1. Introduction

Exposure to environmental odours is one of the major causes of complaints made by residents living near different kinds of industrial and agricultural settlements. Odorous gases typically reach communities at ambient concentrations far below toxicity thresholds. Thus, direct toxicological effects are improbable to occur (Blanes-Vidal et al., 2014a; Palmiotto et al., 2014). However, it has been shown that odour-impacted communities report several negative effects on wellbeing and health. The mechanisms of action remain to be fully elucidated, but there is evidence pointing out that odour annoyance acts as a mediator of exposure–symptoms associations and consequently of complaints (Blanes-Vidal et al., 2014b, 2012; Van Harreveld, 2001).

Different methods have been used internationally to assess odour exposure. Examples include field inspections (CEN, 2016; Van Elst and Delvab, 2016), odour diaries (Sówka et al., 2018), citizen participation (Arias et al., 2018; Sironi et al., 2010), e-noses (Cipriano and Capelli, 2019; Zarra et al., 2019) and dispersion modelling (Brancher et al., 2018; Capelli et al., 2018; Huang and Guo, 2019) Recently, up-to-date reviews of odour impact assessment methods have been presented (Bax et al., 2020; Conti et al., 2020).

Atmospheric dispersion models are used to predict concentrations in

* Corresponding author.
E-mail address: marzio.invernizzi@polimi.it (M. Invernizzi).

https://doi.org/10.1016/j.envint.2020.105990
Received 16 March 2020; Received in revised form 3 June 2020; Accepted 16 July 2020

ambient air around the emission source. These models implement equations to describe the atmospheric processes which affect the transport and the dilution of airborne pollutants. Historically, the dispersion models have been essential to air quality management systems.

Several jurisdictions worldwide commonly assess the odour impact potential of proposals by evaluating the simulated odour concentration statistics against regulatory odour impact criteria (OIC). This represents one of the most common odour analysis approaches used nowadays to determine the acceptability of odour exposure, both for existing and design-phase facilities (Brancher et al., 2017; Capelli et al., 2013). Further, it is the predicted time series of ambient odour concentrations at each receptor location around the emission source that is evaluated by a given odour impact criterion. This evaluation weights if odour impacts of the facility in question can be considered tolerable or not, with regard to odour annoyance. Five factors, designated by the acronym FIDOL (frequency, intensity, duration, offensiveness, and location), are broadly accepted as key dimensions of odour nuisance and are the basis for establishing jurisdictional OIC (Invernizzi et al., 2017; Nicell, 2009).

The vast majority of current dispersion models have been designed to predict pollutant concentrations on an hourly basis, overlooking information on sub-hourly events. Due to the importance of concentration fluctuations to many cases of practical interest, as odour exposure (Dourado et al., 2014; Lo Iacono, 2009; Mahin, 2001; Mussio et al., 2001; Vanderwolf and Zibrowski, 2001), there has recently been an increasing interest in modelling techniques capable of providing information on these kinds of sub-hourly episodes.

The reliability of dispersion models predictions is influenced by different sources of uncertainty. Studies have primarily focused on parameter uncertainty, underlining the influence of the stack exit temperature (Brancher et al., 2020), source temperature (Invernizzi et al., 2019), wind speed (Lucernoni et al., 2017) and operating parameters of unit operations (Invernizzi et al., 2018, 2020), temporal variability of odour emission rates (Brancher et al., 2020; Schauberger et al., 2016) and meteorological input data (Brancher et al., 2019a; Yegnan et al., 2002). Despite its importance, this line of investigation is not taken into account in the present work.

The aim of this study is to compare how the use of a freely available dispersion model, and its short-term concentration evaluation approach, could affect the outcomes of odour impact assessments. This investigation is important because it can shed further light on the range of variation in separation distances. To do so, three different dispersion models have been chosen, following the recommendation of regional guidelines on odour impact assessment presented in Italy (Regione Lombardia, 2012; Regione Piemonte, 2017; Trentino Alto Adige, 2015). Because of the high frequency of calm winds that are typical of northern Italy, Gaussian plume models are not accepted for odour assessment, while Lagrangian-based models are preferred. A *Ceteris Paribus* approach has been followed, to consider the effect and impact of the combination of dispersion model and the dedicated approach for the treatment of sub-hourly peak concentrations.

In particular, the present comparison was performed in three steps. First, the ambient odour exposure, in terms of annual hourly-mean time series values, was calculated using the three dispersion models. From this, the short-term approach of each dispersion model was applied, and another set of results was obtained. Both hourly and short-term concentration time series were evaluated by the odour impact criterion set in Lombardy (Italy) (Regione Lombardia, 2012) to determine separation distances between odour sources and residential areas, as a quantitative value to assess odour annoyance boundaries. Second, separation distance statistics were elaborated, focusing on how much the calculated separation distance increases by considering the short-term instead of the hourly mean concentration. Third, the computed peak-to-mean factors, which are needed to obtain the peak concentration by knowing the hourly mean concentration value, were examined. This comparative analysis has been conducted for two different sites: one located in Austria and one in Italy. A further novelty of this approach lies in a systematic comparison of the results without and with short-term fluctuation treatment, in contrast to other investigations dealing with separation distance results (e. g. Brancher et al., 2019b and c; Oettl and Ferrero, 2017; Piringer et al., 2016b, 2015).

2. State-of-the-art

The odour concentration threshold and the related frequency of exceedance of this threshold (linked to a percentile) are the two main parameters established in the different OIC.

From a statistical point of view, hourly mean concentrations, which are predicted by dispersion models, represent the first moment of the ambient concentration, but they do not include the second moment (variance) (Ferrero et al., 2019). The probability of short-term odour perception is therefore not only related to the mean value, but also to its variability. Odour episodes can, in seconds, cause an odour sensation in the human nose (Mainland and Sobel, 2005). For more information on this concept, the reader is referred for instance to Fig. 1 of Nicell (2009), in which the hourly mean and 12-s concentration trends are compared.

Therefore, the method to evaluate short-term peak concentration (C_p), derived from 1-h mean values (C_m), is often integrated into the definition of regulatory limits for odours (Schauberger et al., 2012). By knowing the so-called "*peak-to-mean factor*" *F*, defined in Eq. (1), and the hourly mean concentration (C_m), it is then possible to estimate, depending on its definition, the value of the peak concentration (C_p).

$$F = \frac{C_p}{C_m} \tag{1}$$

There is no unanimous agreement in the scientific community about the precise definition of this "peak" concentration. The different available definitions of the peak commonly rely on the distribution of the ambient concentration of the single sniff events (Schauberger et al., 2012). That is, the peak can be defined by the mean value and the standard deviation ($C_p = C_m + \sigma$), a percentile (e.g. 90-percentile, 98-percentile or 99-percentile) or the overall maximum value within the hour.

From a physical point of view, the behaviour of concentration fluctuations, due to the turbulent nature of atmospheric boundary layer flows, depends on many parameters. At least one can cite the longitudinal (Mylne and Mason, 1991) and the transversal (Best et al., 2001) distances from the source, and atmospheric stability (Smith, 1973). Further details on the description of the characteristics of atmospheric turbulence, and how it can be considered to treat the peak phenomenon, can be found in Sozzi et al., (2018).

Despite this evidence, the overwhelming majority of the OIC around the world are defined by a fixed, constant value for the peak-to-mean factor *F* (Brancher et al., 2017). For instance, the German Environmental Agency prescribes the use of a constant factor equal to 4 (TA-Luft, 2002) based on the calculation of the 90th percentile of the sub-hourly odour presence. Italian Regional Guidelines agree to use a value of 2.3 (Regione Lombardia, 2012; Regione Piemonte, 2017; Trentino Alto Adige, 2015) but without referring to a specific percentile.

An exception is Austria, where two different approaches have been developed to consider the variability of short-term concentrations. The first one was proposed for the first time by Schauberger et al. (2000) and later improved by considering measured turbulence parameters (Piringer et al., 2016a, 2015). This model is grounded on the widespread correlation of Smith (1973), which evaluates the concentration reached in a short period of time, given the mean concentration over one hour:

$$\frac{C_p}{C_m} = \left(\frac{t_m}{t_p}\right)^u \tag{2}$$

where t_m and t_p represent the long-term (1 h) and short-term averaging time (5 s), respectively, and the non-dimensional exponent u depends on atmospheric stability. Moreover, the experimental data from Mylne and Mason (1991) were exponentially regressed to consider turbulent mixing effects, thereby obtaining an exponential attenuation function for initial peak-to-mean values. More details on this are presented in Section 3.3.2.

More recently, Oettl and Ferrero (2017) proposed an approach based on a simplified version of concentration-variance transport (Ferrero et al., 2017; Manor, 2014). This step would need the assumption of the probability density function (PDF) for the instantaneous odour concentration. Theoretically, by knowing the average and variance values of a variable, and hypothesising its characteristic PDF, it is possible to calculate the value of the percentile of that stochastic variable. This percentile is the value for which a defined frequency in the whole dataset is exceeded. By knowing the hourly mean concentration and the concentration variance field, conjecturing a PDF, which is assumed to represent concentration fluctuations within a 1-h sampling period, and defining a percentile representative of the odour peak event, it is then possible to estimate the peak-to-mean factor as:

$$R_x = \frac{C_x}{\bar{C}} \tag{3}$$

where R_x is the estimated peak-to-mean factor, $\bar{C}$ is the hourly mean concentration and C_x is the peak concentration. More details on this are presented in Section 3.3.3.

We remark that this exceedance frequency (or the percentile), taken for defining R_x, differs from the ones set in OIC: here it is defined as the percentage of exceedances inside the time step of one hour, to determine if in a certain one-hour interval odour perception can be expected. If the peak concentration exceeds the odour concentration threshold of 1 ou_E/m^3, then this one-hour time interval is sometimes called “odour hour” (GOAA, 2008).

3. Material and methods

3.1. Description of sites and meteorological conditions

3.1.1. Meteorological data

Model calculations were performed for two sites. The first one is situated in Groß-Enzersdorf east of Vienna, Austria. The second one is located in Corzano Bargnano in the eastern part of Lombardy, Po valley, Italy. The reference year is 2018. Both sites are mostly characterised by flat terrain, typically farmland. Fig. 1 shows the position of the two sites in Italy and Austria.

For the Austrian site, the surface meteorological observations of 1-h time-steps for wind direction (W_d), wind speed (W_s), air temperature (T), atmospheric pressure (P_{atm}), and relative humidity (RH) were made available by the Central Institute for Meteorology and Geodynamics (ZAMG, Vienna, Austria) for Groß-Enzersdorf GE (48.199°N, 16.559°E). Cloud cover (CC) is not measured at this station, however. The nearest station where CC is recorded is at Schwechat Vienna International Airport LOWW (48.110°N, 16.569°E), located about 10 km from the source. To fulfil the standard quality criteria set by a CALMET meteorological pre-processor, READ62 (Scire et al., 1999), upper air data were obtained from two stations of NOAA/ESRL Radiosonde Database: Wien-Hohe Warte WHW (48.25°N, 16.36°E) and Prostejov LKPJ (49.45°N, 17.13°E), respectively positioned about 16 and 145 km far from the source, respectively.

For the Italian site, the hourly surface meteorological observations of W_d, W_s, T, RH and global radiation (R_g) where provided by the Regional Agency for Environmental Protection (ARPA Lombardia, Milan, Italy) for the station of Corzano Bargnano CB (45.434°N, 10.039°E). The measuring network of ARPA Lombardia do not provide atmospheric pressure and cloud cover data. Due to the scarce influence of atmospheric pressure in the meteorological model (Scire et al., 1999) it has been assumed constant and equal to 1000 mbar. The cloud cover, instead, is needed to calculate micrometeorological parameters. It was obtained from R_g measured data, following the calculation method by Maul (1980). The upper air data were again acquired from NOAA/ESRL Radiosonde Database, in particular from Milano Linate International Airport LIML (45.43°N, 9.28°E), 60 km away from the source. Table 1 recaps meteorological input data used in the present study.

3.1.2. CALMET meteorological pre-processor output

CALMET includes a 3D diagnostic wind field generator. However, input options were set to obtain an uniform wind field, in order to maintain uniformity of meteorological information among CALMET-needing models (CALPUFF and LAPMOD) and GRAL, which uses meteorological information at a single point only.

Fig. 2 reports wind roses obtained for both sites. On the left panels, classical wind roses are shown, while on the right panels the stability roses are depicted. The stability classes were determined by the Pasquill-Gifford-Turner PGT scheme, implemented in CALMET (Scire et al., 1999; US-EPA, 2000) for all the models and sites.

Groß-Enzersdorf in Austria shows high wind speeds, with the two prevailing wind directions northwest (NW) and southeast (SE). Winds characterized as calms (< 0.5 m/s) amount to 0.5% of the observations, with an annual hourly-averaged wind speed of 3.2 m/s. The atmosphere is predominantly stable (36%) with a good portion of neutral conditions (33%).

Corzano Bagnano in Italy has a typical wind regime of the Po valley, showing high amounts of low wind speeds. The main wind direction is west-north-west (WNW) – east-south-east (ESE), with a secondary maximum direction from the northeast (NE), characterized almost only by stable conditions. This kind of atmospheric stability conditions are the most present at this site (46%). Calm winds account for approximately 2.6% of the observations, and the annual hourly-averaged wind speed is 2.0 m/s.

The frequencies of the PGT stability classes for each site are summarised in Table 2.

The simulations were conducted in a 2 km × 2 km flat terrain domain, characterised by uniform agricultural land use. A roughness length, z_0, of 0.25 m was estimated using the pre-processor MAKEGEO (Scire et al., 1999), at both sites.

The height of the receptors was set at 2 m from ground level, as foreseen by the Italian Guidelines (Regione Lombardia, 2012; Regione Piemonte, 2017; Trentino Alto Adige, 2015).

3.2. Odour emission

For all model runs, the same odour emission rate and emission geometry were used (Table 3). In all models, plume rise calculations were enabled. Due to this, an additional source of possible differences in the model outputs, apart from the different peak handling approaches, is introduced by the different algorithms implemented to evaluate plume rise.

To recall, the odour emission rate is kept constant in order to avoid the introduction of an additional variable in this intercomparison. This simplification is common even if it is known that the odour emission rate varies in time (Schauberger et al., 2016) and the variability has an influence on separation distances as well (Brancher et al., 2020).

3.3. Dispersion models

3.3.1. CALPUFF

CALPUFF is a non-steady-state Lagrangian Gaussian puff model containing modules for complex terrain effects, overwater transport, coastal interaction effects, building downwash, wet and dry removal, and simple chemical transformations (Scire et al., 2000). The model implements algorithms to evaluate a transitional plume rise, based on

Fig. 1. Positions of the two sites under investigation. The Austrian site is located in Groß-Enzersdorf, east of Vienna. The Italian site is located in Corzano Bargnano, in the eastern part of Lombardy, Po valley. The two sites are separated by about 600 km. Figure built with Natural Earth, a public domain map dataset (www.naturalearthdata.com).

Table 1
Meteorological stations selected for dispersion simulations.

Site	Station acronym	Type	Coordinates	Elevation ASL (m)	Distance from the source (km)	Hourly metereological parameters
Austria	GE	Surface	48.199°N, 16.559°E	154	0.5	W_d, W_s, T, P_{atm}, RH
	LOWW	Surface	48.110°N, 16.569°E	183	10	CC
	WHW	Upper air	48.25°N, 16.36°E	198	16	W_d, W_s, T, P_{atm}
	LKPJ	Upper air	49.45°N, 17.13°E	216	145	W_d, W_s, T, P_{atm}
Italy	CB	Surface	45.434°N, 10.039°E	92	0.3	W_d, W_s, T, RH, R_g
	LIML	Upper air	45.43°N, 9.28°E	101	60	W_d, W_s, T, P_{atm}

GE: Groß-Enzersdorf; LOWW: Schwechat Vienna International Airport; WHW: Wien-Hohe Warte; LKPJ: Prostejov Airport; CB: Corzano Bargnano; LIML Milano Linate International Ariport; W_d: wind direction; W_s: wind speed; T: air temperature; P_{atm}: atmospheric pressure; RH: relative humidiy; CC: cloud cover; R_g: global solar radiation; ASL: above sea level.

the equations by Briggs (1975). It is one of the most common dispersion models used in Southern European countries such as Spain and Italy (Capelli et al., 2011; Capelli and Sironi, 2018; Murguia et al., 2014; Naddeo et al., 2016; Otero-Pregigueiro and Fernández-Olmo, 2018).

The model is coupled with the meteorological pre-processor CALMET, which calculates the micrometeorological variables, i.e. surface heat flux, friction velocity, Obukhov length, convective velocity scale and mixing height. Dispersion coefficients of the puffs are thus obtained from turbulence parameters.

CALPUFF in its current version does not include any particular

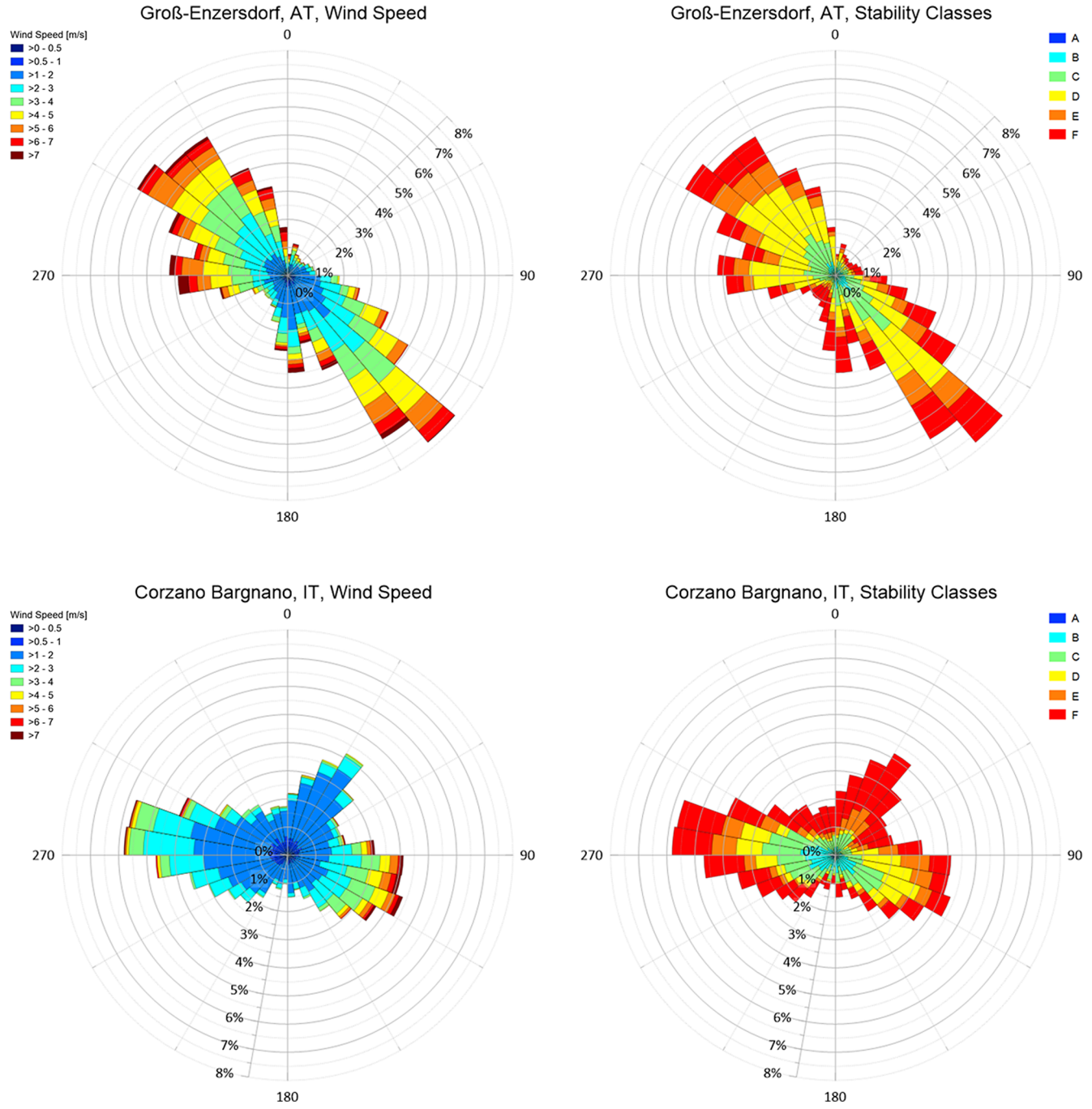

Fig. 2. Wind roses for Groß-Enzersdorf, Austria (top) and Cozano Bargnano, Italy (bottom) for the year 2018. On left side are reported the wind roses with respect to the wind speeds; on the right with respect to the stability classes.

Table 2
Frequency of PGT stability classes obtained by CALMET for both sites.

Stability class	Groβ-Enzersdorf, AT	Corzano Bargnano, IT
A (very unstable)	0.5%	2.1%
B (unstable)	9.7%	16.3%
C (slightly unstable)	19.8%	21.6%
D (neutral)	33.4%	13.7%
E (slightly stable)	13.6%	12.2%
F (stable)	23.1%	34.1%

Table 3
Source data for dispersion calculations.

Stack height	[m]	7.0
Stack diameter	[m]	0.5
Exit velocity	[m/s]	3.0
Exit temperature	[°C]	20
Odour emission rate (OER)	[ou_E/s]	10,000

method to evaluate the sub-hourly concentration. For the elaboration of peak concentrations, CALPUFF can only conduct a simple post-processing, with the tool CALPOST, treating the simulated 1-h concentration field with a constant multiplicative scaling factor.

According to the procedure foreseen by Italian Guidelines on odours (Regione Lombardia, 2012, 2017; Trentino Alto Adige, 2015), to obtain the peak concentration values, the hourly mean concentrations should be multiplied by the constant factor 2.3.

3.3.2. LAPMOD

LAPMOD (Bellasio et al., 2018, 2017) is a 3D, non-stationary Lagrangian particle model that simulates the atmospheric dispersion of inert or radioactive substances, emitted as gases or aerosols. The particles used for the calculation move in the atmosphere, driven by the mean wind (advection) and dispersed by turbulence (dispersion). After the transport simulation, the concentration values are calculated with a kernel algorithm. The plume rise can be estimated in LAPMOD following the approach proposed by Janicke and Janicke (2001) or Webster and Thomson (2002). In the present work, the first algorithm has been set.

The meteorological input of LAPMOD consists of a 3D field of wind and temperature data and 2D fields of turbulence parameters. LAPMOD can directly read the meteorological fields generated by CALMET (version 5.8.5).

Beside conventional pollutants, LAPMOD can simulate the dispersion of odours, implementing also the peak-to-mean approach proposed by (Schauberger et al., 2000).

The initial peak-to-mean factor F_0 is computed with the Eq. (2), while Eq. (4) shows the exponential decrease derived from Mylne and Mason (1991):

$$F = 1 + (F_0 - 1) \bullet exp\left(-0.7317 \frac{T}{T_L}\right) \tag{4}$$

where T is the travel time and T_L is the Lagrangian time scale.

The original approach was implemented in a Gaussian plume model, AODM. In this case, following the nature of the Lagrangian model, the developers introduced some modifications to evaluate these terms. More precisely, T_L is calculated as a weighted average over the particle motion j, during the travel time T, evaluated as sum of the single flying times Δt_j:

$$\frac{T}{T_L} = \frac{T^2}{\sum_j T_{L_{i,j}} \bullet \Delta t_j} = \frac{\left(\sum_j \Delta t_j\right)^2}{\sum_j T_{Li,j} \bullet \Delta t_j} \tag{5}$$

where $T_{Li,j}$ is the Lagrangian time scale for each direction i ($i = [1,2,3]$) at the flying time j. The Lagrangian time scale can be interpreted as an index of correlation between two sequential times of the turbulent motion of a particle. This parameter is different for the three spatial components: for the calculations, the model uses the larger value.

By this point of view, the calculation of LAPMOD cannot be seen as a post-processing based of meteorological conditions and hourly mean concentrations: the short-term concentration predictions are strictly part of the dispersion simulation.

For further specifications about the calculations of Lagrangian time scales in LAPMOD see Section 2.5 of Bellasio et al. (2017).

3.3.3. GRAL

GRAL is a Lagrangian particle model that was developed to deal with the frequent low-wind-speed conditions in the inner-Alpine basins of Austria (Pongratz et al., 2012).

GRAL can compute the flow around obstacles by means of a prognostic microscale wind filed model (Oettl, 2015). Moreover, coupled with the meteorological pre-processor GRAMM (Berchet et al., 2017), it can simulate wind fields for complex terrain. GRAL applies a slightly modified the model of Hurley (2005) to evaluate plume rise.

For the present study, the model has been run in the simplest way, by considering flat terrain and by using the most straightforward way to input meteorological data. Namely, only wind speed and direction and stability classes were inputted to the model.

The GRAL simulation is usually performed in a steady-state mode (the default) by grouping the meteorological data, or in a transient mode by considering all the consecutive time steps.

GRAL was considered in this study because it is the first one which implements the concentration-variance computation reported in Oettl and Ferrero (2017).

To make it compatible with regulatory purposes, the transport equation for the concentration variance, proposed by Hsieh et al. (2007), was simplified, by dropping the advective transport and the turbulent diffusion terms. The derived simplified equation for computing the concentration variance is (Oettl et al., 2018):

$$\frac{\partial \bar{c}^2}{\partial t} = 2\sigma_{ui}^2 T_{Li} \left(\frac{\partial \bar{C}}{\partial x_i}\right)^2 - \frac{\bar{c}^2}{t_d} \tag{6}$$

where $\bar{c}^2$ is the concentration variance, $\bar{C}$ is the mean concentration, σ_{ui}^2, T_{Li}, and t_d are the variances of wind speed fluctuations, the Lagrangian time scales in each direction i ($i = [1,2,3]$), and the dissipation time scale of the concentration variance, respectively.

Moreover, a straightforward equation to estimate the t_d is proposed, avoiding the dependence on source geometry suggested by Ferrero et al. (2017), using the relationship:

$$t_d = 2 \bullet T_{L3} \tag{7}$$

where T_{L3} is the Lagrangian time scale in the vertical direction.

After the computation of the mean concentration field, $\bar{c}^2$ can be computed in the post-processing mode (due to the presence of concentration gradients in Eq. (6)), and so the concentration fluctuation intensity, $i_c = \sigma_c/\bar{C}$, (σ_c is the standard deviation of concentration fluctuations), is obtained.

To evaluate the peak-to-mean values, the authors refer to the definition made by the German regulation (GOAA, 2008) of the odour hour, which is an hour when, at least, in 10% of the time an odour is perceivable. By this, they considered representative the 90th percentile to assess the peak-to-mean factor, R_{90}, in reference from Eq. (3).

As a representative concentration PDF, the model considers a modified 2-parameter Weibull distribution (Forbes et al., 2010). To ensure that R_{90} is rather over than underestimated, R_{90} is multiplied by 1.5 (Oettl, 2019). It has to be mentioned that this approach and the related statistical evaluation originally considered the Weibull PDF to the power of 1.5. Hence, the peak-to-mean factor, R_{90}, is currently within GRAL calculated by the following equation:

$$R_{90} = 1.5 \bullet \left[\frac{(-ln(0.1))^{i_c^{1.086}}}{\Gamma(1 + i_C^{1.086})}\right] \tag{8}$$

where $\Gamma()$ represents the Gamma function (Forbes et al., 2010).

As described in Kuntner and Oettl (2019), to obtain a more reliable result by the concentration-variance transport model, though it takes much higher computational time, GRAL has been run in the transient mode, with the thinnest mesh grid and the highest particle emission rate compatible with the present study.

3.3.4. Comparison of model settings

To give an overview on the parameters used herein, Table 4

Table 4
Parameters and data for the three models. In this study, a desktop computer with 4 parallel processors, 3.6 GHz CPU and 16 GB RAM was used for performing the required numerical simulations.

Model	Version	Grid size [m]	Internal parametrization of Emission	Computational wall- clock time [h]
CALPUFF	5.8.5	20	Defined by the model (~99 puffs/h)	2
LAPMOD	June 2017	20	3600 part/h	2
GRAL	19.1	5	720,000 part/h	210

summarises information on the CALPUFF, LAPMOD and GRAL model runs.

3.4. Odour impact criteria (OIC) and statistical analysis

After the simulation run, the time series of ambient odour concentration are evaluated by odour impact criteria (OIC). By this means, separation distances can be determined for a certain protection level. OIC can be simply defined by an odour concentration threshold and the percentile compliance level of this threshold. In Italy, there is currently no national guideline or law prescribing a specific concentration threshold that shall not be exceeded. However, the different regional guidelines prescribe to follow essentially the same methodological approach.

According to the Regional Guideline of Lombardy (Regione Lombardia, 2012), impact maps must be drawn and they should report peak odour concentration values at the 98th percentile, on an annual basis. The evaluation must consider the territory, the presence of potential receptors on it, and the characteristics of the background, taking into account that (Regione Lombardia, 2012):

- at 1 ou_E/m^3, 50% of the population perceives the odour;
- at 3 ou_E/m^3, 85% of the population perceives the odour;
- at 5 ou_E/m^3, 90–95% of the population perceives the odour.

Although this guideline underlines that in the scientific literature there is no unanimous agreement about the definition of a reasonable value, a constant factor for the peak-to-mean ratio, equal to 2.3, is recommended (Regione Lombardia, 2012). This odour impact criterion has been considered in the present work. To recall, separation distances at the 98th percentile of sub-hourly peak odour concentrations have been determined using different approaches for each selected dispersion model:

– For CALPUFF, the Italian constant factor of 2.3 was used (Regione Lombardia, 2012);
– For LAPMOD, the approach implemented by Schauberger et al. (2000) was used;
– For GRAL, the concentration variance model by Oettl and Ferrero (2017) was used.

To recall, the results are analysed and presented by evaluating so-called separation distances. Such distances denote the contour lines (isoplethes) of an ambient concentration threshold at a fixed exceedance probability of this threshold. These are parameters of the selected odour impact criterion described above.

For the statistical analyses performed herein, we first measured the resultant separation distances in a direction-dependent manner. This procedure was realised for each 10° sector, which gives 36 distances for every case. Second, from such measures, we attempted to formally quantify to what extent the introduction of different algorithms to estimate short-term concentrations affects the outcomes.

A simple and useful means to do so is the direction-dependent scaling factor, which is here defined as the ratio of the separation distances due to fluctuation treatment (considering short-term concentrations) and the separation distances without fluctuation treatment (based on hourly mean concentrations).

We also computed four statistical metrics: mean bias (MB), normalised mean bias (NMB), root mean squared error (RMSE) and normalised mean squared error (NMSE). The formulas of such widely used metrics have been defined in several earlier studies (Bennett et al., 2013; Chang and Hanna, 2004; Jackson et al., 2019). Classically, these and other statistical metrics, have been used to assess model prediction skill on the basis of predicted data, observed data and number of prediction–observation pairs. Two models can also be compared by assuming a reference situation, as done in the present work. Our assumed reference situation was the hourly mean-related separation distances. This reference was compared with separation distances based on the short-term odour concentration. Differently than for scaling factors, the statistical metrics bring the direction-dependent separation distances down to a number. We underline that this statistical analysis does not have the aim to compare modelled and “true” values, but to furnish numerical quantitative information for investigating how the consideration of the different short-term approaches can affect separation distance results.

The selected metrics were computed using R version 3.6.1 (R Core Team, 2019) with the *openair* package (Carslaw and Ropkins, 2012).

4. Results

4.1. Contour maps

Fig. 3 and Fig. 4 show the obtained contour maps for the Austrian and the Italian site, respectively. In each of these figures, CALPUFF results (left) are compared to LAPMOD (centre) and GRAL results (right). The results of the dispersion calculations on a 1-hour basis are shown in the upper panel. The lower panel reports the contour lines evaluated by considering the different short-term concentration evaluation approaches (Section 3.3). It is worthy to first compare the mean concentration fields, neglecting any short-term algorithms. Potential differences in results can then be mainly attributed to the different model physics, basically the different plume rise formulations, but also the differences in the parameter settings (Table 4).

Starting by considering the hourly mean ambient concentrations for the Austrian site in Fig. 3 and comparing them against Fig. 2, it is possible to note that the wind distribution is a main element driving the shape of the contour maps. The elongation of the lines tends to be greater towards the prevailing winds, e.g. southeast (SE) and northwest (NW) for all the models: this behaviour is well represented by the 1 ou_E/m^3 green lines. Considering the two other odour protection levels, represented by yellow (3 ou_E/m^3) and red lines (5 ou_E/m^3), some noticeable differences appear. While for CALPUFF and LAPMOD these impact lines appear quite close to each other and at low distances from the source, the GRAL model evaluates a considerable area for the value of 3 ou_E/m^3, whereas for 5 ou_E/m^3, almost no value is obtained.

By turning to the lower panel of Fig. 3, showing the peak ambient concentrations for Groß-Enzersdorf, we can deduce that the short-term concentrations enlarge the impacted area for all concentrations considered. All the lines still exhibit a prolonged impacted distance coherent with the most frequently observed wind direction. Nevertheless, it should be pointed out that, while for GRAL the increase of the impacted area seems homogeneous for all directions, CALPUFF displays a slightly more important elongation towards north (N), and LAPMOD reports a more pronounced enlargement towards east (E) and northwest (NW).

At the Italian site, the hourly mean values (upper panel of Fig. 4), in particular the ones obtained from CALPUFF and LAPMOD, still evidence the influence of the wind distribution (Fig. 2, bottom). By the way, it turns out a major extension of the 1 ou_E/m^3 green line towards south-west (SW). On the other hand, GRAL shows a more uniform extent of the impacted area for all the directions. Considering the lower protection levels (3 ou_E/m^3 and 5 ou_E/m^3), the results show a trend similar to the Austrian site: the two lines are close to each other both for CALPUFF and LAPMOD, while GRAL estimates a significant region affected by the value of 3 ou_E/m^3, although negligible sectors reach the value of 5 ou_E/m^3.

Regarding the separation distances obtained by considering short-term concentrations (Fig. 4, bottom panel), the lengthening of the impacted area in the main and secondary wind directions is relevant also in this case. CALPUFF shows the largest area where 1 ou_E/m^3 is exceeded, with the maximum elongation of about 1 km from the source in the south-west (SW) direction. The 1 ou_E/m^3 line displays comparable

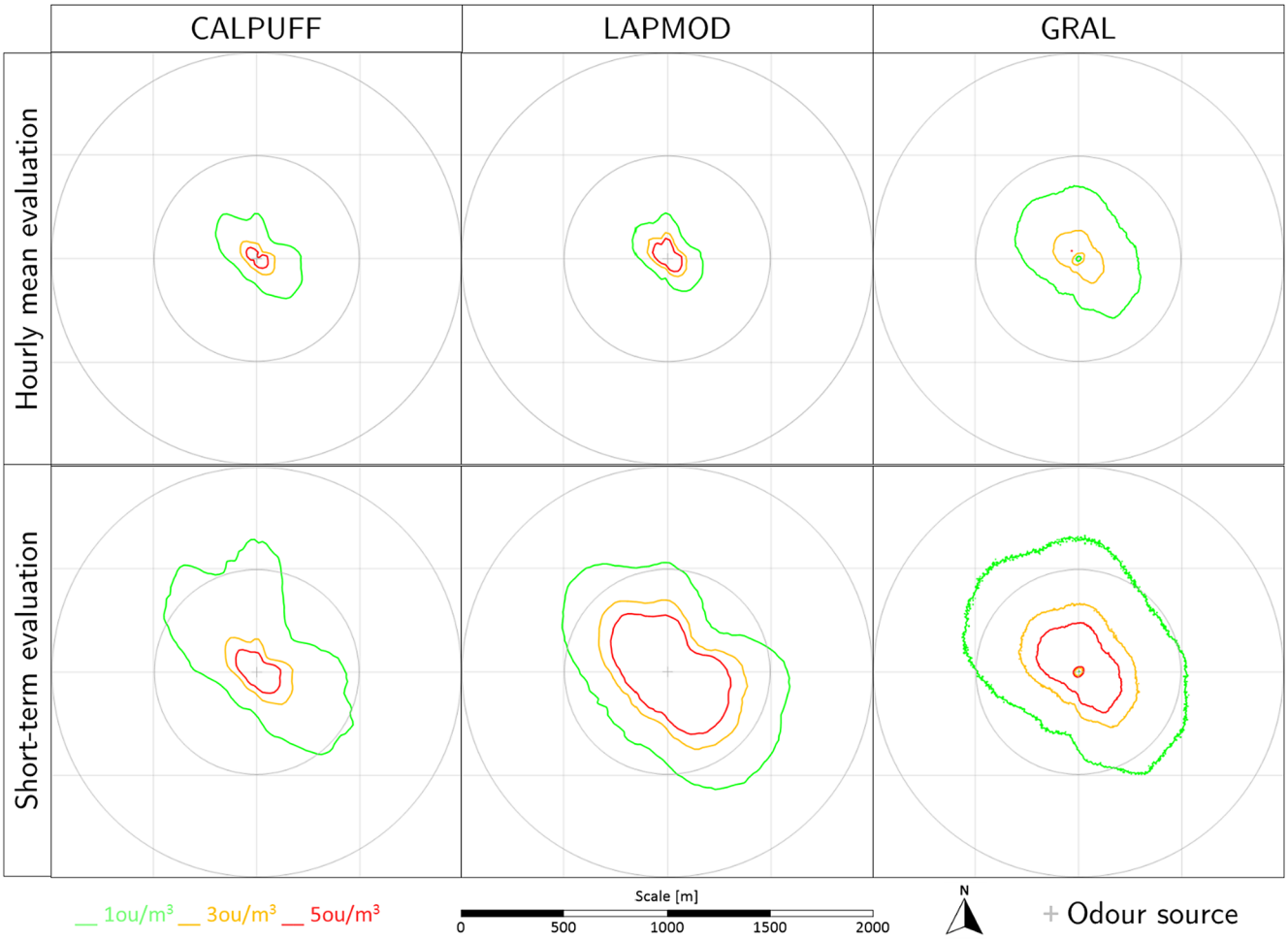

Fig. 3. Contour maps at the Austrian site for all model runs. The upper contour maps show the hourly means (e.g. no fluctuation treatment is considered), while the lower maps consider the short-term calculations of each dispersion model. The centre of the plots indicates the odour source.

results in the dominant wind directions WNW-ESE for all three models. Proceeding to the yellow (3 ou_E/m^3) and red (5 ou_E/m^3) lines, both GRAL and LAPMOD return a more important growth of the impacted area than CALPUFF. A remarkable finding is the reshaping of the maps due to the short-term considerations. While the use of CALPUFF and GRAL exhibit an enlargement of the contours, the shape of the odour maps produced by LAPMOD changes completely, resulting in a major impacted area in the wind-dominant WNW-ESE directions and a huge elongation in the first quad (from north to east).

For the high protection level of 1 ou_E/m^3 and peak ambient concentration, the contour line shows remarkable differences between the Austrian and the Italian sites: whereas, at the Austrian site, CALPUFF shows the smallest area of this threshold exceedance, at the Italian site it shows the largest area, compared to the two other models. For 3 and 5 ou_E/m^3, LAPMOD returns the largest affected area, at both sites.

4.2. Separation distance intercomparison

Fig. 5 and Fig. 6 report the direction-dependent separation distances for the three considered concentration thresholds. The former refers to the Austrian and the latter to the Italian site. On the left panels of these figures, separation distances obtained by the hourly mean concentration data are presented, and on the right panels those with short-term treatment.

In order to facilitate the analysis of results for all directions, a minimum separation distance from the source was considered. Due to the use of Lagrangian instead of Gaussian plume models, (for the latter, Piringer et al. (2016b) for example considered a lower limit of 100 m), we selected the arbitrary value of 25 m for this minimum. This means that separation distances $\leq$25 m were set to 25 m as a lower limit in this evaluation. However, this assumption resulted in only a few cases to be adjusted (essentially for high odour concentration threshold when using GRAL without any short-term consideration).

Focusing on the results of the hourly mean values first, the graphs of the Austrian site (Fig. 5, left panels) show parallel separation distances for 1 and 3 ou_E/m^3 for GRAL and LAPMOD, with GRAL estimating the highest separation distances (up to 400 m towards the north direction), followed by CALPUFF and LAPMOD. For the 3 ou_E/m^3 level, the lines tend to get closer, overlapping in different sectors (e.g. south-east SE), with GRAL again showing the highest values of about 150 m.

On the contrary, for the highest odour concentration threshold (5 ou_E/m^3), the largest separation distances are calculated by LAPMOD (nearly 100 m), followed by CALPUFF. GRAL reaches this concentration threshold only in one direction (NW); all other separation distances were set to the assumed minimum value of 25 m.

Discussing the results gained with short-term concentrations (right panels of Fig. 5) for the lowest odour concentration threshold (1 ou_E/m^3), GRAL still estimates the highest separation distance (~650 m) towards north, while the estimates of CALPUFF and LAPMOD are similar, for this direction. Besides, GRAL and LAPMOD show comparable results for all other directions except NE. CALPUFF instead gives the lowest separation distances in almost all other directions except towards north. Looking at the higher odour concentration thresholds, the lines tend to slip away from each other with a replicable performance:

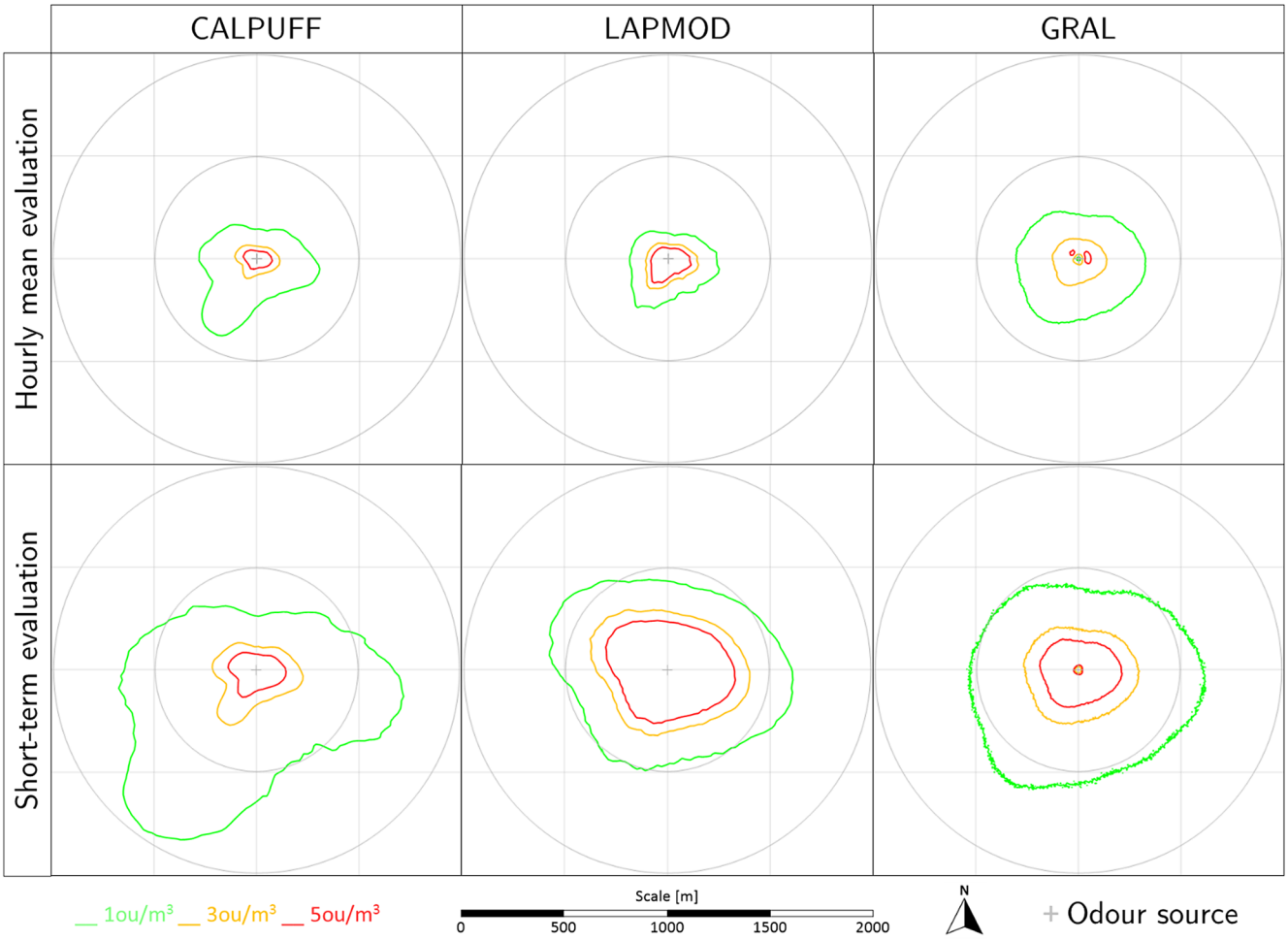

Fig. 4. Contour maps at the Italian site for all model runs. The upper contour maps show the hourly means (e.g. no fluctuation treatment is considered), while the lower maps consider the short-term calculations of each dispersion model. The centre of the plots indicates the odour source.

the higher the concentration considered, the more LAPMOD exhibits high results (except for transport towards NE), followed by GRAL and finally by CALPUFF (with differences up to and even more than a factor 3).

Passing to the Italian site, Fig. 6, the outcomes from the hourly mean concentration (left panels) of 1 ou_E/m^3 for GRAL and LAPMOD run in parallel, with GRAL delivering again the highest values. CALPUFF-related separation distances, with the exception of the SW peak reaching 400 m, lie in between. For 3 ou_E/m^3, the GRAL and LAPMOD lines are very close, ranging from 80 to 150 m, with CALPUFF giving the lowest estimates. The results for 5 ou_E/m^3 are comparable to the Austrian site (Fig. 5): GRAL estimates separation distances for this concentration threshold only for a few directions, while LAPMOD calculates the highest separation distances for this criterion, with values up to 120 m for transport towards SW.

Analysing the separation distances linked to short-term results, for 1 ou_E/m^3 (upper right panel of Fig. 6), GRAL and LAPMOD display a similar trend with various overlapping portions. CALPUFF, instead, shows a large directional variation between 250 m towards N and a peak in the SSW direction (900 m).

Regarding the highest impact concentration threshold, the tendency seen at the Austrian site is even clearer: LAPMOD gives the highest separation distances, while CALPUFF provides the lowest values. GRAL, neglecting the SSW CALPUFF's peak at 3 ou_E/m^3, exhibits an intermediate behaviour. The separation distances calculated by using CALPUFF and LAPMOD differ up to a factor of 3, for most directions.

4.3. Separation distance statistics

In order to evaluate to what extent the introduction of different short-term algorithms can affect the obtained separation distances, a useful metric is the ratio between separation distances with (short-term) and without (hourly mean) fluctuation treatment. We refer to this ratio herein as separation distance scaling factor. Accordingly, Fig. 7 presents the results for both sites dispersion models (CALPUFF, left panel; LAPMOD, central panel; GRAL, right panel) and concentration thresholds under investigation (1 ou_E/m^3 in green, 3 ou_E/m^3 in yellow and 5 ou_E/m^3 in red). Again, separation distances $\leq$25 m were set to 25 m as a lower limit for this evaluation. We note that such scaling factors have the disadvantage of being sensitive to small changes in direction-dependent separation distance values. Even though, they can deliver useful information as shown next.

CALPUFF exhibits a fairly constant separation distance scaling factor at both sites for all the considered odour levels, which ranges from about 2–2.5. Some peaks can be seen towards south-west (SW) for the Italian site and in north direction for the Austrian one, reaching maximum values of 3.

The results obtained by LAPMOD are much more diverse. The spread of scaling factors is much larger if we compare the Austrian against the Italian site. The obtained scaling factors are more compact for the lowest odour level (1 ou_E/m^3) where values from 3 to 4 are obtained, and tend to spread more by increasing the considered odour concentration, obtaining top values higher than 10 for the odour concentration threshold of 5 ou_E/m^3.

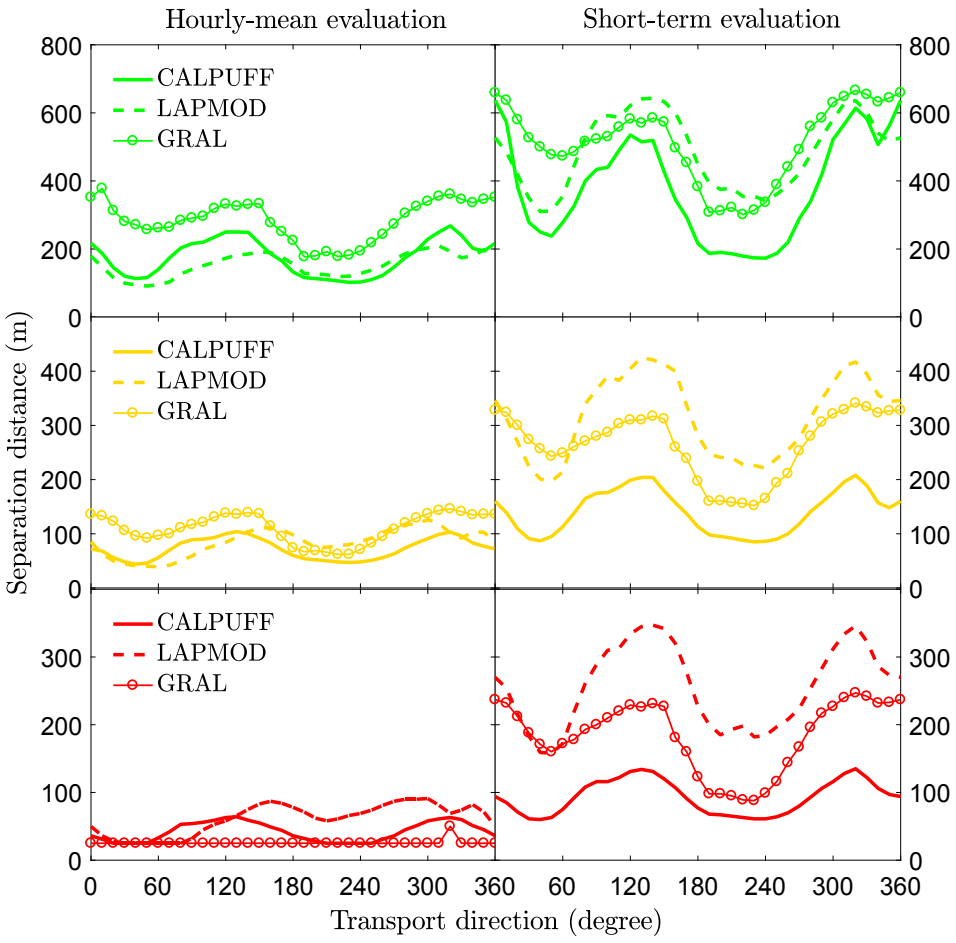

Fig. 5. Austrian site: Direction-dependent separation distances considering the hourly mean evaluation (left panels) and the short-term evaluation (right panels). Legend denotes the dispersion models according to each concentration threshold (1 ou_E/m^3 in green, 3 ou_E/m^3 in yellow and 5 ou_E/m^3 in red) of the selected odour impact criterion. (For interpretation of the references to colour in this figure legend, the reader is referred to the web version of this article.)

For the GRAL model, the separation distance scaling factors obtained for 1 and 3 ou_E/m^3 are very close to a value of 2, independent of the study site. This is similar to the CALPUFF results. For 5 ou_E/m^3 the results are completely different and more similar to LAPMOD. This is due to the fact that GRAL, as mentioned in Section 4.1, estimates only few directions where this odour concentration is reached for the 98th percentile for the hourly mean concentration. This leads to a very frequent assumption of the minimum value of 25 m for the separation distance, invalidating the achievement of a consistent result for the separation distance-scaling factor.

Table 5 and Table 6 show the outcomes of the model evaluation statistics for the Austrian and Italian sites, respectively. In accordance with the previous sections, the comparison was carried out for the three dispersion models and the three protection levels (concentration thresholds) of the designated odour impact criterion.

The normalised metrics NMB and NMSE are dimensionless, while the others, MB and RMSE, match the units of our response (in m). The ideal value for MB, NMB, RMSE and NMSE, when comparing the obtained data with the expected ones, is zero. The obtained results of the selected metrics are all positive, indicating "overestimation". This was expected once the ambient odour concentration predictions by considering short-term fluctuations tend to increase, with direct consequences to the separation distance determination.

The computed statistical metrics provide the following results:

- The lower the concentration threshold, the greater the differences in separation distances due to the hourly mean evaluation against the short-term one. For instance, when using CALPUFF with 1 $ou_E\ m^{-3}$ for the Austrian site, the RMSE was 223 m, while with 5 $ou_E\ m^{-3}$, the RMSE is reduced to 52 m. This detection suggests that the prediction of annoyance via modelling criteria (that is, OIC) is more vulnerable to show more pronounced differences for lower concentration thresholds when a short-term evaluation is attempted;
- Regarding the dispersion models and their methods of estimating short-term concentrations, for both sites, the method applied with CALPUFF returned the overall smallest differences in separation distances. In contrast, the method applied with LAPMOD returned the overall largest differences.

We can also summarise the following model-related results when comparing the Austrian site against the Italian site:

- CALPUFF: higher metric results, meaning larger differences in separation distances, at the Italian than at the Austrian site, for all concentration thresholds;
- LAPMOD: higher metric results at the Austrian site for all concentration thresholds;
- GRAL: slightly higher metric results at the Italian site for 1 $ou_E\ m^{-3}$, while the metric results were slightly higher at the Austrian site for 3 and 5 $ou_E\ m^{-3}$.

Therefore, our work reveals non-trivial odour assessment outcomes which are contingent upon the dispersion model and site, emphasised further by the use of the same source emission data for all cases.

4.4. Distribution of peak-to-mean factors in the domain

Based on the methodologies outlined in Section 3.3, it is possible to estimate the time-averaged peak-to-mean factors in the whole model domain of the two investigated sites. These values are not the

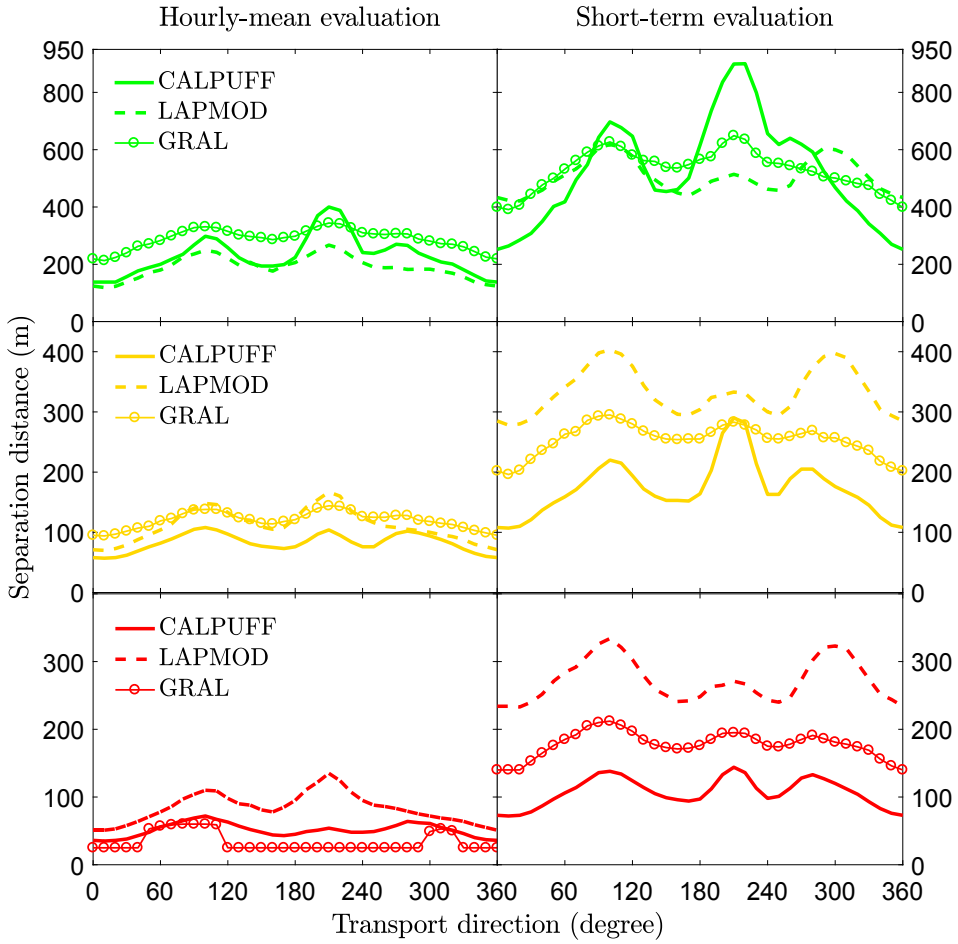

Fig. 6. Italian site: Direction-dependent separation distances considering the hourly mean evaluation (left panels) and the short-term evaluation (right panels). Legend denotes the dispersion models according to each concentration threshold (1 ou_E/m^3 in green, 3 ou_E/m^3 in yellow and 5 ou_E/m^3 in red) of the selected odour impact criterion. (For interpretation of the references to colour in this figure legend, the reader is referred to the web version of this article.)

individual ones used in each simulation time-step. They represent the average value of the overall simulation time (i.e., 1 year), which has been calculated in each receptor point within the domain for the two reported variable short-term approaches used in LAPMOD and GRAL.

Fig. 8 reports the average values of the peak-to-mean factors calculated by LAPMOD for the two sites are reported. In this case, LAPMOD does not calculate these values by default. Therefore, in order to obtain the peak-to-mean factors, a specific MATLAB algorithm has been implemented to evaluate the ratio between the peak and hourly concentration values, for each single simulation time step and for each receptor of the grid. Accordingly, the reported values are the average values at each point of the grid. Besides, GRAL autonomously elaborates the average R_{90} gridded values when the concentration variance post processing is run. Such results are reported in Fig. 9.

The peak-to-mean values computed by LAPMOD exhibit very different values for the two sites: at the Austrian site, the peak-to-mean factors range from 1 to 7, showing the higher factors in the main wind directions (SE-NW). On the contrary, the calculated values for the Italian site are much higher, ranging from 2 to 14. In this case, the result does not seem directly linked to the main wind directions: the highest peak-to-mean factors are located in the first quad, between east and north.

In general, at both sites, a decrease of the average peak-to-mean factors with distance from the source is observed.

Considering the GRAL short-term approach, the obtained average R_{90} (Fig. 9) values are much steadier in the whole domain, pointing out, almost widespread, avearages between 2.2 and 2.6. The highest R_{90}-averaged values are found near the source, but rarely reaching average values higher than 3. This behaviour is further confirmed by the spatially-averaged R_{90} values reported in Table 7.

Even if the values reported in Table 7 represent overall means (temporally and spatially) and thus give only a rough indication of the altogether behaviour of the considered models, they can be useful to understand which model is providing more conservative outcomes.

The highest values of average peak-to-mean factors are obtained with LAPMOD, in particular for the Italian site, while the lowest are drawn by CALPUFF. GRAL mostly provides intermediate results, which are similar to the constant Italian factor of 2.3 used with CALPUFF.

5. Discussion

5.1. Metereological and stability data

ZAMG's measurement site at Groß Enzersdorf is well equipped with several meteorological instruments for testing and calibration. A mast is instrumented with two ultrasonic anemometers at 10 m height, namely, an orthogonal 2D (*uSonic-2 Wind*, Metek Gmbh) and a non-orthogonal 3D (*uSonic-3 Scientific,* Metek Gmbh). The sonics are mounted pointing into the dominant winds at the end of a boom that extends from the side of the mast. Whereas the wind rose in Fig. 2 is due to two-axis sonic data, the wind rose shown in (Brancher et al., 2020) stems from the three-axis sonic data. A visual comparison of the wind frequency distribution depicted by the wind rose reported in this work and the one by Brancher et al. (2020), shows an overall good agreement between them.

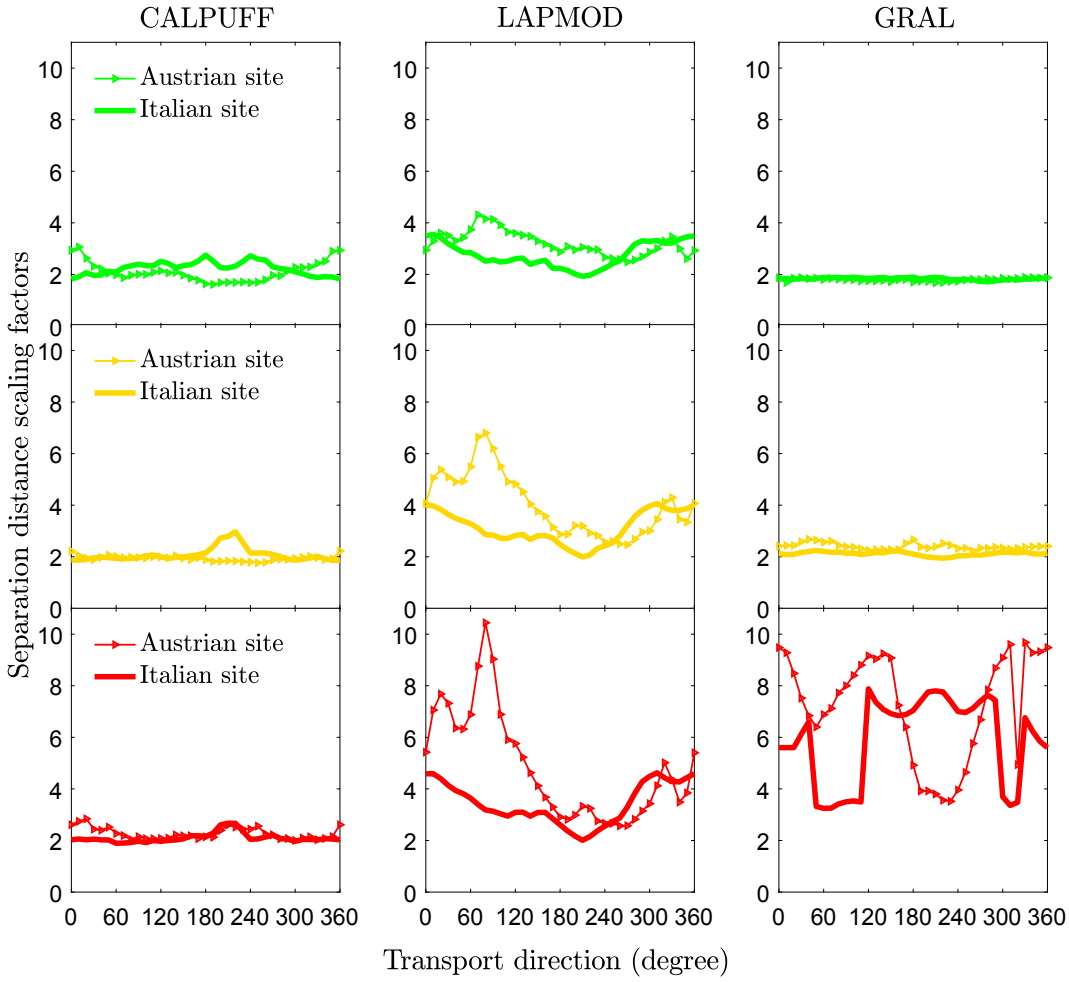

Fig. 7. Separation distance scaling factors to quantify potential differences in separation distances due to the consideration of short-term concentrations against hourly means. Results are shown for the two sites under investigation by dispersion model (CALPUFF, left panel; LAPMOD, central panel; GRAL, right panel) and concentration threshold (1 ou_E/m^3 in green, 3 ou_E/m^3 in yellow and 5 ou_E/m^3 in red) of the selected odour impact criterion. (For interpretation of the references to colour in this figure legend, the reader is referred to the web version of this article.)

Table 5
Austrian site (Groß-Enzersdorf): model evaluation statistics comparing hourly mean separation distances against short-term separation distances using the mean bias (MB), the normalised mean bias (NMB), the root mean squared error (RMSE), and normalised mean squared error (NMSE).

Dispersion model	Concentration threshold [$ou_E\ m^{-3}$]	*n*	MB	NMB	RMSE	NMSE
CALPUFF	1	36	199	1.1	223	0.7
	3	36	68	0.9	72	0.5
	5	36	51	1.2	52	0.6
LAPMOD	1	36	333	2.2	343	1.5
	3	36	231	2.7	240	2.1
	5	36	194	3.2	202	2.5
GRAL	1	36	226	0.8	233	0.4
	3	36	154	1.4	157	0.8
	5	36	157	6.1	165	5.7

Table 6
Italian site (Corzano Bargnano): model evaluation statistics comparing hourly mean separation distances against short-term separation distances using the mean bias (MB), the normalised mean bias (NMB), the root mean squared error (RMSE), and normalised mean squared error (NMSE).

Dispersion model	Concentration threshold [$ou_E\ m^{-3}$]	*n*	MB	NMB	RMSE	NMSE
CALPUFF	1	36	297	1.3	319	0.8
	3	36	91	1.1	97	0.6
	5	36	57	1.1	58	0.6
LAPMOD	1	36	317	1.7	321	1.1
	3	36	221	2.0	224	1.3
	5	36	188	2.2	191	1.6
GRAL	1	36	242	0.8	244	0.4
	3	36	134	1.1	135	0.6
	5	36	145	4.3	146	3.5

However, some differences in both the horizontal mean wind direction and speed arise. A dedicated study that aims to compare those fundamentally different sonic designs will be needed to determine whether these preliminary differences that have been detected can be considered rather significant, and, if so, to identify their potential causes. For instance, well-known sonic anemometers shortcomings, such as probe-induced flow distortion effects, typically due to transducer shadowing and mounting structures, have been long acknowledged to cause measurement errors (Frank et al., 2020; Horst et al., 2015; Huq et al., 2017; Kaimal et al., 1990; Mauder et al., 2020; Mauder and Zeeman, 2018; Peña et al., 2019).

The outcome that atmospheric stability is predominantly stable at the Austrian site for 2018 dataset is contingent on the classified stability scheme (Pasquill-Gifford-Turner PGT) used in the present work. Again for this same site, in a previous study (Brancher et al., 2020), the Obukhov length was calculated from the 3D sonic data showing that

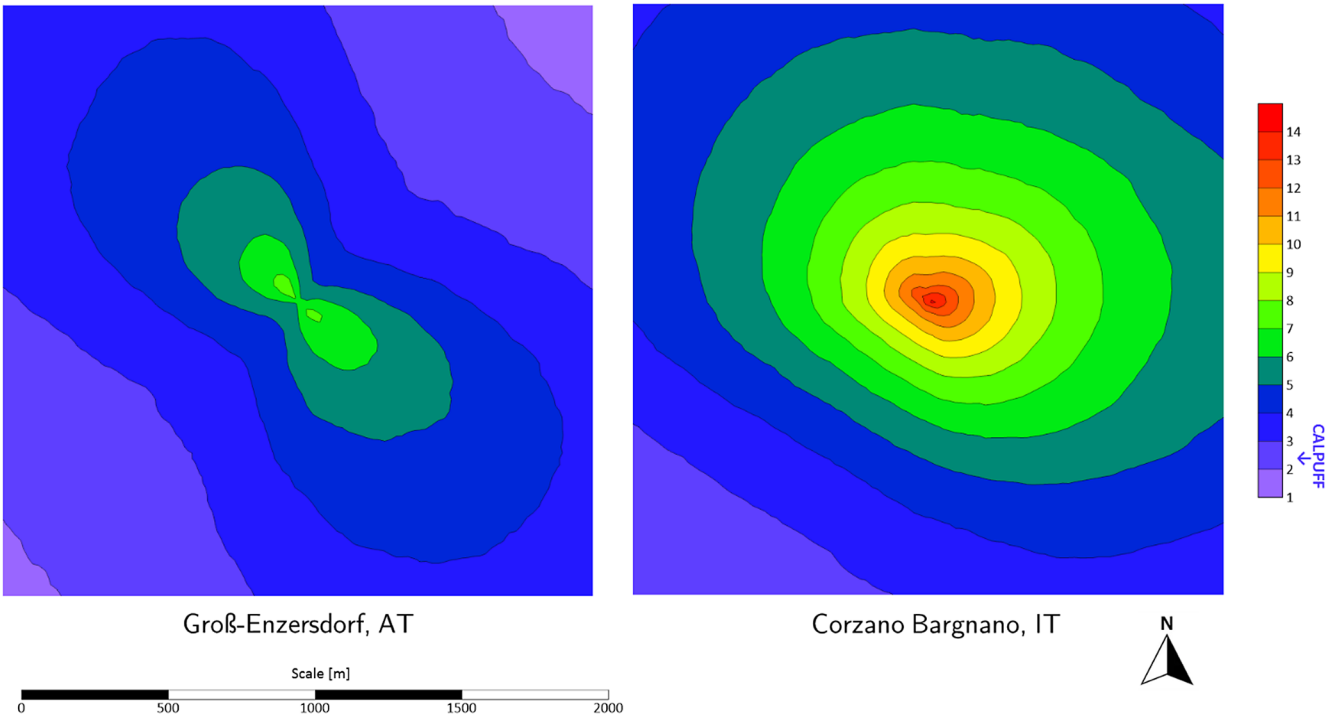

Fig. 8. Average peak-to-mean factors in the whole domain calculated by LAPMOD, for the Austrian site (on the left) and for the Italian site (on the right). Aside the color bar is reported the level of the constant peak-to-mean factor used for CALPUFF model, equal to 2.3.

atmospheric stability was mostly neutral, and then stable. For the sake of additional comparison with the PGT scheme, we also applied the German Klug-Manier scheme (VDI 3782 Part 6, 2017) to the 2D sonic data collected at the Austrian site. The resultant stability conditions were once more mostly neutral, followed by stable cases. Differences in the occurrence frequencies of stability classes between these two classified schemes can be expected. They are mainly related to

Table 7
Average peak-to-mean factors for the overall simulation period (annual-hourly time series for 2018) in the whole domain (2 km × 2 km).

Study site	CALPUFF (constant)	LAPMOD	GRAL
Groß-Enzersdorf, AT	2.3	3.7	2.5
Corzano Bargnano, IT	2.3	5.4	2.5

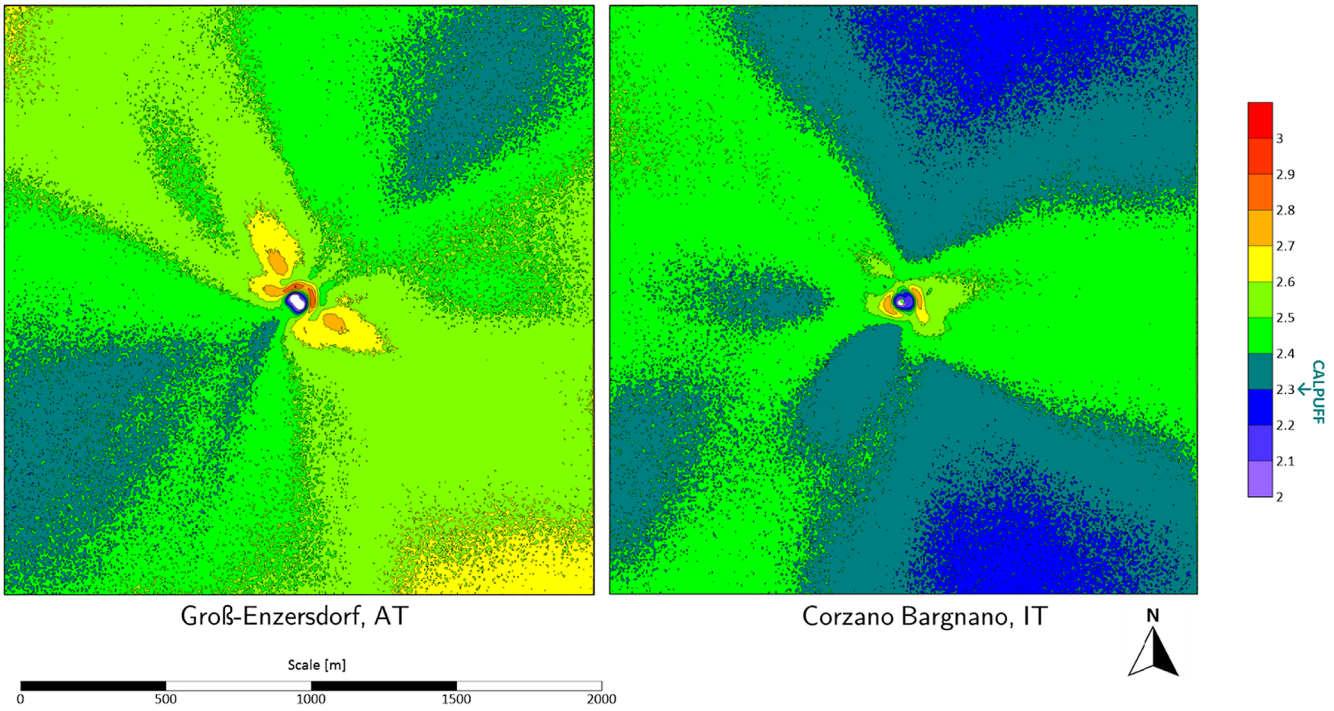

Fig. 9. Average peak-to-mean factors (R_{90}) in the whole domain calculated by GRAL, for the Austrian site (left panel) and for the Italian site (right panel). Aside the color bar is reported the level of the constant peak-to-mean factor used for CALPUFF model, equal to 2.3.

modifications in the handling of cloud amount and wind speed data within the schemes, especially different stability class limits and day-night and seasonal attributions.

5.2. Odour dispersion simulations

Direction-dependent separation distances can be enforced by regulatory authorities for decision making on odour annoyance. This approach easily provides information to all stakeholders about the area within which odour annoyance can be foreseen. The separation distance can be considered a parameter that overlaps the different contributions to the emission and the dispersion: source characteristics, odour emission rate, transport and dilution by atmospheric phenomena, and the OIC considered (Brancher et al., 2019b).

It is challenging to compare the results of different dispersion models directly. Even if here the model input data have been kept as homogeneous as possible, the authors are aware that it is very difficult to have identical model input data and model settings. For example, the different frameworks of the selected dispersion models, the treated physical phenomena and the model settings (see Table 4) cause input alterations. The methodology applied here aimed at maintaining the most reasonable set up, following the recommendations of each model users guide, compatible with the calculation time and the limits of the models.

The wind direction is the most important driver for separation distance determination. All of the hourly mean results, depicted in contour maps reported in Section 4.1, denote a similarity with the wind roses reported in Fig. 2. Moreover, the atmospheric stability, in particular for Corzano Bargnano, well displays its effect: the 1 ou_E/m^3 green line major extension is in south-west (SW) direction, even if this is not a prevalent direction at the location. The combination of frequent wind directions with stable conditions is a pre-requisite for larger separation distances (Piringer et al., 2016b).

By looking at the upper contour maps reported in Section 4.1 and on the values of separation distances on the left of the figures exposed in Section 4.2, it's possible to see that the simulation of the hourly mean value shows comparable results among the three models. The most important difference arises in the near-field of the source: LAPMOD, in particular, estimates high concentration values in the near-field with a fast decrease with distance. Besides, GRAL shows a different behaviour, with high concentration values not being reached in the proximity of the source (e.g. no contour lines for 5 ou_E/m^3), but the low concentrations are spread over longer distances.

At least part of these differences in hourly-mean evaluation results, differences can be linked to the different plume rise schemes implemented by the models. While the method of LAPMOD (Janicke and Janicke, 2001) seems to keep the particles more gathered near to the emission point, equations within GRAL (Hurley, 2005) provide a more pronounced "umbrella effect". To a lesser extent, the referred differences can be attributable to the varying grid sizes for the two models (Table 4).

Proceeding to the evaluation of the short-term ambient concentration, it is clear that a specific peak evaluation algorithm poses a strong influence on the size and shape of the impacted area. This is particularly true for the LAPMOD model, for which the separation distance scaling factor (Fig. 7) reached values of 10 (for the Italian site). These pronounced changes in results are coherent with the data obtained for the peak-to-mean value maps (Fig. 8). The strong differences between the two sites are due to the different meteorological conditions, in special the atmospheric stability situations. The initial peak-to-mean factor, evaluated by Eq. (2), varies with a stability-dependent exponent. In Table 8, this exponent u and the initial peak-to-mean values, F_0, for the different stability classes, considering the peak and averaging times of the present study (t_m = 3600 s and t_p = 5 s), calculated by LAPMOD, are reported (Bellasio and Bianconi, 2017).

Table 8
Stability-dependent exponent u for the calculation of initial peak-to-mean ratios, F_0, in LAPMOD.

	A	B	C	D	E	F
u	0.65	0.65	0.52	0.35	0	0
F_0	72	72	31	10	1	1

The Italian site is characterized by 18% of unstable situations (PGT classes A and B), while at the Austrian one, only 10% of all situations are unstable. This means that the amount of situations with high initial peak-to-mean values is much higher at the Italian site, increasing the average value all over the domain, as shown in Table 7.

Comparing Fig. 8 against Fig. 4 (Italian site), it is easy to see that the distortion of the impacted area evaluated by LAPMOD when considering the short-term is due to the peak-to-mean model, which provides higher results in the first quad.

The LAPMOD-retrieved peak-to-mean factors are much higher and show a much slower decrease with distance from the source than reported in Piringer et al. (2016a, 2015). Accordingly, the results obtained by LAPMOD have a completely different behaviour, showing average values of 5 even at 1 km from the source. This can be explained by the different way to derive the travel time T and the Lagrangian time scale T_L compared to the original approach used in the AODM model (see Sections 2 and 3.3.2). LAPMOD calculates these values as reported in Eq. (5) using the scheme of Hurley and Physick (1993). The approach originally published in Schauberger et al. (2000) considered the travel time correlated to the linear distance from the source x, $T = x/u$, with u the wind speed, and the Lagrangian time scale $T_L = \sigma^2/\varepsilon$, where σ^2 and ε are the mean variance of the wind velocity components in the three directions and the turbulent kinetic energy dissipation rate, respectively. This means that different formulations of travel time and Lagrangian time scale can lead to different results in the peak-to-mean factors from Eq. (4).

On the other hand, GRAL estimates R_{90} values that do not vary greatly, as reported in Fig. 9, resulting for both sites in spatial-averaged values of 2.5. From this, we can consider that the concentration-variance transport method, is less site-dependent than the LAPMOD approach.

Moreover, on average GRAL, with the concentration-variance transport method, reports spatially averaged peak-to-mean factors similar to the constant factor of 2.3 used with CALPUFF. The contour map of the GRAL model shows an enlargement of the impacted area for both sites, but without a significant distortion. This is also well represented in the almost constant values of the separation distance scaling factors, shown in Fig. 7. This does not hold true for the odour impact criterion of 5 ou_E/m^3 (bottom right panel of Fig. 7). The reason is that GRAL, as mentioned in Section 4.1, estimates only few directions where this odour concentration threshold is reached for the 98th percentile of the hourly mean ambient concentration run. This leads to the very frequent assumption of the minimum value of 25 m for the separation distance. For this very particular context, the higher the concentration thresholds of OIC, the more uncertain are the estimates of the scaling factors and thus the separation distances. The concentration threshold of 1 ou_E/m^3 delivers the most reliable results both for separation distances and separation distances scaling factors

It is noted that the presented results are linked to one compliance percentile (98th) or exceedance probability (2%) and continuous emissions from a point source. According to previous studies (Brancher et al., 2019b and references therein), potential differences in separation

distances, caused by a variety of factors other than peak-to-mean methods, can be awaited to be reduced for lower percentiles, particularly the 90th.

6. Conclusions

The consideration of short-term peak concentrations is crucial to obtain more reliable results when using a dispersion model for odour assessments. In this regard, here a comparative study of modelling methods for odour impact assessment has been elaborated. The focus was put upon three atmospheric dispersion models (CALPUFF, LAPMOD and GRAL) and their different approaches to consider short-term concentrations.

The analysis considers two sites, located in Austria and Italy, and is based an on odour impact criterion enforced in some Italian regions: the 98th percentile level of exceedance is calculated for three concentration threshold levels (1, 3 and 5 ou_E/m^3). Contour lines and separation distances were then obtained and compared both considering hourly mean and short-term concentrations.

The calculation times were different: whereas CALPUFF and LAPMOD needed a similar time for the calculations (2 h), GRAL, by selecting high definition simulation parameters and the transient mode, took much more time than the others, by a factor of 1:100. These durations are anyway strictly dependent on the model parameters, here exposed in Table 4.

A better accordance in hourly mean concentration has been found for high protection levels then for the low protections levels: the different model plume rise algorithms may affect the results more in the vicinity of the source, leading to different outcomes.

By accounting for short-term concentrations, the impacted area and the obtained separation distances were as expected expanded in all cases, when compared to the hourly mean concentration results (Fig. 3 and Fig. 4). The introduction of the peak calculations makes the results from the three models less directly comparable. While the CALPUFF and GRAL outcomes are more similar for the Italian than the Austrian site, LAPMOD estimates very high short-term concentration values, above all at short distances from the source. This fact is confirmed by the calculated average peak-to-mean factors: the average values for LAPMOD rarely reach the lower limit of 1 (Fig. 8), only at distances further away from the source at the Austrian site, unlike is present in literature (Piringer et al., 2015, 2016a). On the other hand, GRAL provides a narrow interval of peak-to-mean factors, with an average value of 2.5 when considering the whole simulation period and domain. Such a result is similar with the Italian constant factor of 2.3 used with CALPUFF.

The present investigation provides practical information on how an atmospheric dispersion model and its method to calculate short-term concentrations can affect the conclusions of an odour impact assessment. Here no field measurements were undertaken. Future studies could focus on different peak-to-mean approaches, while using the same ensemble-averaged dispersion algorithm, and on concentration-fluctuation measurements, to compare simulations against field or wind tunnel experiments.

CRediT authorship contribution statement

Marzio Invernizzi: Conceptualization, Methodology, Software, Data curation, Writing - original draft, Visualization. **Marlon Brancher:** Conceptualization, Software, Formal analysis, Data curation, Writing - review & editing, Visualization. **Selena Sironi:** Investigation, Resources, Supervision. **Laura Capelli:** Investigation, Writing - review & editing, Supervision. **Martin Piringer:** Methodology, Investigation, Writing - review & editing, Supervision. **Günther Schauberger:** Methodology, Investigation, Resources, Writing - review & editing, Supervision.

Declaration of Competing Interest

The authors declare that they have no known competing financial interests or personal relationships that could have appeared to influence the work reported in this paper.

Acknowledgements

The authors want to thank ZAMG and ARPA Lombardia for providing the meteorological datasets. A further thanks goes to Roberto Sozzi, who was crucial to fully explore the theoretical aspects at the base of this study. Marlon Brancher was supported by the Austrian Science Fund (FWF) in the framework of the Lise Meitner Programme [project number M 2548-N29].

References

Arias, Rosa, Capelli, Laura, Diaz, Carlos, 2018. A new methodology based on citizen science to improve environmental odour management. Chem. Eng. Trans. 68, 7–12. https://doi.org/10.3303/CET1868002.

Bax, C., Sironi, S., Capelli, L., 2020. How can odors be measured? An overview of methods and their applications. Atmosphere (Basel) 11, 92.

Bellasio, R., Bianconi, R., 2017. LAPMOD - User's manual Enviroware.

Bellasio, R., Bianconi, R., Mosca, S., Zannetti, P., 2018. Incorporation of numerical plume rise algorithms in the Lagrangian particle model LAPMOD and validation against the Indianapolis and Kincaid datasets. Atmosphere (Basel). 9. https://doi.org/10.3390/atmos9100404.

Bellasio, R., Bianconi, R., Mosca, S., Zannetti, P., 2017. Formulation of the Lagrangian particle model LAPMOD and its evaluation against Kincaid SF6 and SO2 datasets. Atmos. Environ. 163, 87–98. https://doi.org/10.1016/J.ATMOSENV.2017.05.039.

Bennett, N.D., Croke, B.F.W., Guariso, G., Guillaume, J.H.A., Hamilton, S.H., Jakeman, A.J., Marsili-Libelli, S., Newham, L.T.H., Norton, J.P., Perrin, C., Pierce, S.A., Robson, B., Seppelt, R., Voinov, A.A., Fath, B.D., Andreassian, V., 2013. Characterising performance of environmental models. Environ. Model. Softw. 40, 1–20. https://doi.org/10.1016/j.envsoft.2012.09.011.

Berchet, A., Zink, K., Oettl, D., Brunner, J., Emmenegger, L., Brunner, D., 2017. Evaluation of high-resolution GRAMM-GRAL (v15.12/v14.8) NO2 simulations over the city of Zürich, Switzerland. Geosci. Model Dev. 10, 3441–3459. https://doi.org/10.5194/gmd-10-3441-2017.

Best, P.R., Lunney, K.E., Killip, C.A., 2001. Statistical elements of predicting the impact of a variety of odour sources. Water Sci. Technol.

Blanes-Vidal, V., Bælum, J., Nadimi, E.S., Løfstrøm, P., Christensen, L.P., 2014a. Chronic exposure to odorous chemicals in residential areas and effects on human psychosocial health: Dose–response relationships. Sci. Total Environ. 490, 545–554. https://doi.org/10.1016/j.scitotenv.2014.05.041.

Blanes-Vidal, V., Bælum, J., Schwartz, J., Løfstrøm, P., Christensen, L.P., 2014b. Respiratory and sensory irritation symptoms among residents exposed to low-to-moderate air pollution from biodegradable wastes. J. Expo. Sci. Environ. Epidemiol. 24, 388–397. https://doi.org/10.1038/jes.2014.20.

Blanes-Vidal, V., Suh, H., Nadimi, E.S., Løfstrøm, P., Ellermann, T., Andersen, H.V., Schwartz, J., 2012. Residential exposure to outdoor air pollution from livestock operations and perceived annoyance among citizens. Environ. Int. 40, 44–50. https://doi.org/10.1016/J.ENVINT.2011.11.010.

Brancher, M., Griffiths, K.D., Franco, D., de Melo Lisboa, H., 2017. A review of odour impact criteria in selected countries around the world. Chemosphere 168, 1531–1570. https://doi.org/10.1016/j.chemosphere.2016.11.160.

Brancher, M., Knauder, W., Piringer, M., Schauberger, G., 2020. Temporal variability in odour emissions: To what extent this matters for the assessment of annoyance using dispersion modelling. Atmos. Environ. X 5, 100054. https://doi.org/10.1016/J.AEAOA.2019.100054.

Brancher, M., Piringer, M., Franco, D., Belli Filho, P., De Melo Lisboa, H., Schauberger, G., 2019a. Assessing the inter-annual variability of separation distances around odour sources to protect the residents from odour annoyance. J. Environ. Sci. (China) 79, 11–24. https://doi.org/10.1016/j.jes.2018.09.018.

Brancher, M., Piringer, M., Grauer, A.F., Schauberger, G., 2019b. Do odour impact criteria of different jurisdictions ensure analogous separation distances for an equivalent level of protection? J. Environ. Manage. 240, 394–403. https://doi.org/10.1016/j.jenvman.2019.03.102.

Brancher, M., Piringer, M., Grauer, A.F., Schauberger, G., 2018. Characterization of year-to-year variability of separation distances between odour sources and residential areas to avoid annoyance. Chem. Eng. Trans. 68, 19–24. https://doi.org/10.3303/CET1868004.

Briggs, G.A., 1975. Lectures on air pollutants and environmental impact analysis. Plume rise Predict. Am. Meteorol. Soc., Bost. 59–111.

Capelli, L., Grande, M., Intini, G., Sironi, S., 2018. Comparison of field inspections and dispersion modelling as a tool to estimate odour emission rates from landfill surfaces. Chem. Eng. Trans. 68, 187–192. https://doi.org/10.3303/CET1868032.

Capelli, L., Sironi, S., 2018. Combination of field inspection and dispersion modelling to estimate odour emissions from an Italian landfill. Atmos. Environ. 191, 273–290. https://doi.org/10.1016/J.ATMOSENV.2018.08.007.

Capelli, L., Sironi, S., Del Rosso, R., Céntola, P., Rossi, A., Austeri, C., 2011. Odour impact assessment in urban areas: case study of the city of Terni. Procedia Environ. Sci. 151–157. https://doi.org/10.1016/j.proenv.2011.03.018.
Capelli, L., Sironi, S., Del Rosso, R., Guillot, J.-M., 2013. Measuring odours in the environment vs. dispersion modelling: a review. Atmos. Environ. 79, 731–743. https://doi.org/10.1016/j.atmosenv.2013.07.029.
Carslaw, D.C., Ropkins, K., 2012. openair — An R package for air quality data analysis. Environ. Model. Softw. 27–28, 52–61. https://doi.org/10.1016/j.envsoft.2011.09.008.
CEN, 2016. EN 16841:2016 Ambient air - Determination of odour in ambient air by using field inspection - Part 1: Grid method.
Chang, J.C., Hanna, S.R., 2004. Air quality model performance evaluation. Meteorol. Atmos. Phys. 87, 167–196. https://doi.org/10.1007/s00703-003-0070-7.
Cipriano, D., Capelli, L., 2019. Evolution of electronic noses from research objects to engineered environmental odour monitoring systems: a review of standardization approaches. Biosensors 9. https://doi.org/10.3390/bios9020075.
Conti, C., Guarino, M., Bacenetti, J., 2020. Measurements techniques and models to assess odor annoyance: a review. Environ. Int. 134, 105261. https://doi.org/10.1016/J.ENVINT.2019.105261.
Dourado, H., Santos, J.M., Reis, N.C., Mavroidis, I., 2014. Development of a fluctuating plume model for odour dispersion around buildings. Atmos. Environ. 89, 148–157. https://doi.org/10.1016/J.ATMOSENV.2014.02.053.
Ferrero, E., Manor, A., Mortarini, L., Oettl, D., 2019. Concentration fluctuations and odor dispersion in Lagrangian models. Atmosphere (Basel). 11. https://doi.org/10.3390/atmos11010027.
Ferrero, E., Mortarini, L., Purghè, F., 2017. A simple parametrization for the concentration variance dissipation in a Lagrangian single-particle model. Boundary-Layer Meteorol. 163, 91–101. https://doi.org/10.1007/s10546-016-0218-x.
Forbes, C., Evans, M., Hastings, N., Peacock, B., 2010. Statistical Distributions, Fourth. ed. https://doi.org/10.1002/9780470627242.
Frank, J.M., Massman, W.J., Chan, W.S., Nowicki, K., Rafkin, S.C.R., 2020. Coordinate rotation-amplification in the uncertainty and bias in non-orthogonal sonic anemometer vertical wind speeds. Boundary-Layer Meteorol. 175, 203–235. https://doi.org/10.1007/s10546-020-00502-3.
GOAA, 2008. Guideline on Odour in Ambient Air (GOAA) - Detection and Assessment of Odour in Ambient Air.
Horst, T.W., Semmer, S.R., Maclean, G., 2015. Correction of a non-orthogonal, three-component sonic anemometer for flow distortion by transducer shadowing. Boundary-Layer Meteorol. 155, 371–395. https://doi.org/10.1007/s10546-015-0010-3.
Hsieh, K.-J., Lien, F.-S., Yee, E., 2007. Numerical modeling of passive scalar dispersion in an urban canopy layer. J. Wind Eng. Ind. Aerodyn. 95, 1611–1636. https://doi.org/10.1016/J.JWEIA.2007.02.028.
Huang, D., Guo, H., 2019. Dispersion modeling of odour, gases, and respirable dust using AERMOD for poultry and dairy barns in the Canadian Prairies. Sci. Total Environ. 690, 620–628. https://doi.org/10.1016/j.scitotenv.2019.07.010.
Huq, S., De Roo, F., Foken, T., Mauder, M., 2017. Evaluation of probe-induced flow distortion of campbell CSAT3 sonic anemometers by numerical simulation. Boundary-Layer Meteorol. 165, 9–28. https://doi.org/10.1007/s10546-017-0264-z.
Hurley, P., Physick, W., 1993. A skewed homogeneous lagrangian particle model for convective conditions. Atmos. Environ. Part A. Gen. Top. 27, 619–624. https://doi.org/10.1016/0960-1686(93)90219-O.
Hurley, P.J., 2005. The air pollution model (TAPM) Version 3. Part 1: Technical description. CSIRO Atmos. Res. Tech. Pap. 57.
Invernizzi, M., Bellini, A., Miola, R., Capelli, L., Busini, V., Sironi, S., 2019. Assessment of the chemical-physical variables affecting the evaporation of organic compounds from aqueous solutions in a sampling wind tunnel. Chemosphere 220, 353–361. https://doi.org/10.1016/J.CHEMOSPHERE.2018.12.124.
Invernizzi, M., Capelli, L., Sironi, S., 2017. Proposal of odor nuisance index as urban planning tool. Chem. Senses 42. https://doi.org/10.1093/chemse/bjw103.
Invernizzi, M., Ilare, J., Capelli, L., Sironi, S., 2018. Proposal of a method for evaluating odour emissions from refinery storage tanks. Chem. Eng. Trans. 68, 49–54. https://doi.org/10.3303/CET1868009.
Invernizzi, M., Teramo, E., Busini, V., Sironi, S., 2020. A model for the evaluation of organic compounds emission from aerated liquid surfaces. Chemosphere 240. https://doi.org/10.1016/j.chemosphere.2019.124923.
Jackson, E.K., Roberts, W., Nelsen, B., Williams, G.P., Nelson, E.J., Ames, D.P., 2019. Introductory overview: Error metrics for hydrologic modelling – A review of common practices and an open source library to facilitate use and adoption. Environ. Model. Softw. 119, 32–48. https://doi.org/10.1016/j.envsoft.2019.05.001.
Janicke, U., Janicke, L., 2001. A three-dimensional plume rise model for dry and wet plumes. Atmos. Environ. 35, 877–890. https://doi.org/10.1016/S1352-2310(00)00372-1.
Kaimal, J., Gaynor, J., Zimmerman, H., Zimmerman, G., 1990. Minimizing flow distortion errors in a sonic anemometer. Boundary-Layer Meteorol. 53, 103–115.
Kuntner, M., Oettl, D., 2019. GRAL workshop [WWW Document]. URL https://www.youtube.com/watch?v=LjeqXrPol-Q.
Lo Iacono, G., 2009. Application of Rice's theory to recurrence statistics of concentration fluctuations in dispersing plumes. Environ. Fluid Mech. 9, 341–357. https://doi.org/10.1007/s10652-008-9099-y.
Lucernoni, F., Capelli, L., Busini, V., Sironi, S., 2017. A model to relate wind tunnel measurements to open field odorant emissions from liquid area sources. Atmos. Environ. 157, 10–17. https://doi.org/10.1016/j.atmosenv.2017.03.004.
Mahin, T.D., 2001. Comparison of different approaches used to regulate odours around the world. Water Sci. Technol. 44, 87–102. https://doi.org/10.2166/wst.2001.0514.
Mainland, J., Sobel, N., 2005. The sniff is part of the olfactory percept. Chem. Senses 31, 181–196. https://doi.org/10.1093/chemse/bjj012.
Manor, A., 2014. A stochastic single-particle Lagrangian model for the concentration fluctuations in a plume dispersing inside an urban canopy. Boundary-Layer Meteorol. 150, 327–340. https://doi.org/10.1007/s10546-013-9871-5.
Mauder, M., Eggert, M., Gutsmuths, C., Oertel, S., Wilhelm, P., Voelksch, I., Wanner, L., Tambke, J., Bogoev, I., 2020. Comparison of turbulence measurements by a CSAT3B sonic anemometer and a high-resolution bistatic Doppler lidar. Atmos. Meas. Tech. 13, 969–983. https://doi.org/10.5194/amt-13-969-2020.
Mauder, M., Zeeman, M.J., 2018. Field intercomparison of prevailing sonic anemometers. Atmos. Meas. Tech. 11, 249–263. https://doi.org/10.5194/amt-11-249-2018.
Maul, P.R., 1980. Atmospheric Transport of Sulphur Compound Pollutants. Imperial College London.
Murguia, W., Pagans, E., Barclay, J., Scire, J., 2014. Case study: a comparison of predicted Odour exposure levels in barcelona using CALPUFF lite, CALPUFF NoObs and CALPUFF Hybrid model. Chem. Eng. Trans. 40, 31–36. https://doi.org/10.3303/CET1440006.
Mussio, P., Gnyp, A.W., Henshaw, P.F., 2001. A fluctuating plume dispersion model for the prediction of odour-impact frequencies from continuous stationary sources. Atmos. Environ. 35, 2955–2962. https://doi.org/10.1016/S1352-2310(00)00419-2.
Mylne, K.R., Mason, P.J., 1991. Concentration fluctuation measurements in a dispersing plume at a range of up to 1000 m. Q. J. R. Meteorol. Soc. 117, 177–206. https://doi.org/10.1002/qj.49711749709.
Naddeo, V., Zarra, T., Oliva, G., Chiavola, A., Vivarelli, A., 2016. Environmental odour impact assessment of landfill expansion scenarios: case study of Borgo Montello (Italy). Chem. Eng. Trans. 54, 73–78. https://doi.org/10.3303/CET1654013.
Nicell, J.A., 2009. Assessment and regulation of odour impacts. Atmos. Environ. 43, 196–206. https://doi.org/10.1016/j.atmosenv.2008.09.033.
Oettl, D., 2019. Private communications.
Oettl, D., 2015. Evaluation of the revised Lagrangian particle model GRAL against wind-tunnel and field observations in the presence of obstacles. Boundary-Layer Meteorol. 155, 271–287. https://doi.org/10.1007/s10546-014-9993-4.
Oettl, D., Ferrero, E., 2017. A simple model to assess odour hours for regulatory purposes. Atmos. Environ. 155, 162–173. https://doi.org/10.1016/j.atmosenv.2017.02.022.
Oettl, D., Kropsch, M., Mandl, M., 2018. Odour assessment in the vicinity of a pig-fatting farm using field inspections (EN 16841–1) and dispersion modelling. Atmos. Environ. 181, 54–60. https://doi.org/10.1016/j.atmosenv.2018.03.029.
Otero-Pregigueiro, D., Fernández-Olmo, I., 2018. Use of CALPUFF to predict airborne Mn levels at schools in an urban area impacted by a nearby manganese alloy plant. Environ. Int. 119, 455–465. https://doi.org/10.1016/J.ENVINT.2018.07.005.
Palmiotto, M., Fattore, E., Paiano, V., Celeste, G., Colombo, A., Davoli, E., 2014. Influence of a municipal solid waste landfill in the surrounding environment: toxicological risk and odor nuisance effects. Environ. Int. 68, 16–24. https://doi.org/10.1016/j.envint.2014.03.004.
Peña, A., Dellwik, E., Mann, J., 2019. A method to assess the accuracy of sonic anemometer measurements. Atmos. Meas. Tech. 12, 237–252. https://doi.org/10.5194/amt-12-237-2019.
Piringer, M., Knauder, W., Petz, E., Schauberger, G., 2016a. Determining separation distances to avoid odour annoyance with two models for a site in complex terrain. Chem. Eng. Trans. 54, 7–12. https://doi.org/10.3303/CET1654002.
Piringer, M., Knauder, W., Petz, E., Schauberger, G., 2016b. Factors influencing separation distances against odour annoyance calculated by Gaussian and Lagrangian dispersion models. Atmos. Environ. 140, 69–83. https://doi.org/10.1016/j.atmosenv.2016.05.056.
Piringer, M., Knauder, W., Petz, E., Schauberger, G., 2015. A comparison of separation distances against odour annoyance calculated with two models. Atmos. Environ. 116, 22–35. https://doi.org/10.1016/j.atmosenv.2015.06.006.
Pongratz, T., Öttl, D., Uhrner, U., 2012. Documentation of the Lagrangian Particle Model GRAL (Graz Lagrangian Model) 111.
R Core Team, 2019. R: A language and environment for statistical computing. R Foundation for Statistical Computing, Vienna, Austria.
Regione Lombardia, 2012. D.g.r. 15 febbraio 2012 - n. IX/3018 - Determinazioni generali in merito alla caratterizzazione delle emissioni gassose in atmosfera derivanti da attività a forte impatto odorigeno.
Regione Piemonte, 2017. D.g.r. 9 gennaio 2017, n. 13-4554. L.R. 43/2000 - Linee guida per la caratterizzazione e il contenimento delle emissioni in atmosfera provenienti dalle attività ad impatto odorigeno.
Schauberger, G., Piringer, M., Petz, E., 2016. Influence of the variability of the odour emission rate on the separation distance shown for the Irish odour impact criterion. Chem. Eng. Trans. 54, 193–198. https://doi.org/10.3303/CET1654033.
Schauberger, G., Piringer, M., Petz, E., 2000. Diurnal and annual variation of the sensation distance of odour emitted by livestock buildings calculated by the Austrian odour dispersion model (AODM). Atmos. Environ. 34, 4839–4851. https://doi.org/10.1016/S1352-2310(00)00240-5.
Schauberger, G., Piringer, M., Schmitzer, R., Kamp, M., Sowa, A., Koch, R., Eckhof, W., Grimm, E., Kypke, J., Hartung, E., 2012. Concept to assess the human perception of odour by estimating short-time peak concentrations from one-hour mean values. Reply to a comment by Janicke et al. Atmos. Environ. 54, 624–628. https://doi.org/10.1016/J.ATMOSENV.2012.02.017.
Scire, J.S., Robe, F.R., Fernau, M.E., Yamartino, R.J., 1999. A User's Guide for the CALMET Meteorological Model, version 5.0.
Scire, J.S., Strimaitis, D.G., Yamartino, R.J., 2000. A User's Guide for the CALPUFF Dispersion Model. Earth Tech. Inc 521. https://doi.org/10.1016/0196-9781(85)90178-0.
Sironi, S., Capelli, L., Céntola, P., Del Rosso, R., Pierucci, S., 2010. Odour impact assessment by means of dynamic olfactometry, dispersion modelling and social participation. Atmos. Environ. 44, 354–360. https://doi.org/10.1016/j.atmosenv.2009.

10.029.
Smith, M., 1973. Recommended Guide for the Prediction of the Dispersion of Airborne Effluents, No, 68-31123, New York. Am. Soc. Mech. Eng.
Sówka, I., Miller, U., Bezyk, Y., Nych, A., Grzelka, A., Dabrowski, L., 2018. Application of field inspections and odour observation diaries in the assessment of air quality and odour in urban areas. E3S Web Conf. 45, 86. https://doi.org/10.1051/e3sconf/20184500086.
Sozzi, R., Bolignano, A., Sironi, S., Capelli, L., 2018. Reflections on odour concentration fluctuations and nuisance. Chem. Eng. Trans. 68, 199–204. https://doi.org/10.3303/CET1868034.
TA-Luft, 2002. Technische Anleitung Zur Reinhaltung der Luft. First General Administrative Regulation Pertaining the Federal Immission Control Act. Federal Ministry for Environment, Nature Conservation and Nuclear Safety.
Trentino Alto Adige, G. provinciale, 2015. Linee guida per la caratterizzazione, l'analisi e la definizione dei criteri tecnici e gestionali per la mitigazione delle emissioni delle attività ad impatto odorigeno.
US-EPA, 2000. Meteorological Monitoring Guidance for Regulatory Modeling Applications. Epa-454/R-99-005 171.
Van Elst, T., Delvab, J., 2016. The European Standard prEN 16841–2 (Determination of odour in ambient air by using field inspection: plume method): a review of 20 years experience with the method in Belgium. Chem. Eng. Trans. 54.
Van Harreveld, A.P., 2001. From odorant formation to odour nuisance: new definitions for discussing a complex process. Water Sci. Technol. 44, 9–15.
Vanderwolf, C., Zibrowski, E.M., 2001. Pyriform cortex β-waves: odor-specific sensitization following repeated olfactory stimulation. Brain Res. 892, 301–308. https://doi.org/10.1016/S0006-8993(00)03263-7.
VDI 3782 Part 6, 2017. Environmental Meteorology - Atmospheric Dispersion Models - Determination of Klug/Manier Dispersion Categories. Verein Deutscher Ingenieure.
Webster, H.N., Thomson, D.J., 2002. Validation of a Lagrangian model plume rise scheme using the Kincaid data set. Atmos. Environ. 36, 5031–5042. https://doi.org/10.1016/S1352-2310(02)00559-9.
Yegnan, A., Williamson, D.G., Graettinger, A.J., 2002. Uncertainty analysis in air dispersion modeling. Environ. Model. Softw. 17, 639–649. https://doi.org/10.1016/S1364-8152(02)00026-9.
Zarra, T., Galang, M.G., Ballesteros, F., Belgiorno, V., Naddeo, V., 2019. Environmental odour management by artificial neural network – A review. Environ. Int. 133, 105189. https://doi.org/10.1016/J.ENVINT.2019.105189.